Excitonic Screening in Semiconductors

Johannes de Boor

UNIVERSITÄT ROSTOCK

Thesis for Diploma

Excitonic Screening in Semiconductors

Johannes de Boor

Rostock, September 2006

prepared at
Universität Rostock, Institut für Physik
AG Festkörpertheorie

Supervisor: Prof. Dr. Henneberger

Address: Universität Rostock
Institut für Physik
18051 Rostock
Tel: +49 381 498-6926
Internet: http://www.physik3.uni-rostock.de

Supervisor's email: klaus.henneberger@uni-rostock.de
Author's email: johannes.de-boor@uni-rostock.de

Preface

Semiconductors

semi-...?

You probably won't trust too much in a *semi-* friend, and I do not believe that Michael Schumacher would have much success in a *semi*-Ferrari, however and surprisingly, there are plenty of things you can do with a *semi*-conductor.
You can fabricate diodes and transistors from them ("boring"), the graphic card in your computer is made of semiconductors ("That's useful!"), you can call someone via an orbital satellite standing two steps behind you, and you can manufacture optical devices like laser pointers from them. Or, even cooler, you can construct your own laser sword with a semiconductor laser and give Darth Vader a damn good fight ("Crazy Stuff!!").
Well, for all these and a lot of other applications you have to understand semiconductor physics. And the more exciting the applications are meant to be, the better you have to understand the physics behind them. It is the aim of this thesis to shed light onto a small island within the infinite and dark blue ocean of semiconductor physics, suffering from the storm of quantum-statistical-many-body problems. Or, to be a bit more concrete, the focus of this thesis is an improved description of screening.

Contents

1 Motivation and General Remarks **9**

2 Theory **11**
2.1 General Properties of an Excited Semiconductor 11
2.2 Classical Theory of Screening 14
2.3 Many-Body Effects and Green's Functions 16
2.3.1 Introduction to Green's Functions 17
2.3.2 Semiconductor Bloch Equations 21
2.3.3 The Debye Approximation for the Selfenergy 24
2.4 Ideal and Interacting Coulomb Plasma 25
2.4.1 Partially Ionised System: Saha's Equation 26

3 The Polarisation Function **35**
3.1 Polarisation Function of an Ideal Plasma 35
3.1.1 Discussion and Results 35
3.1.2 Limiting Cases 38
3.1.3 Plasmons and Plasmon Pole Approximation 40
3.2 The One-Particle Polarisation Function
for a Nonideal Plasma 42
3.3 The Excitonic Polarisation Function 45
3.3.1 Introduction and Discussion 45
3.3.2 Numerical Results 51

4 The Diagonal Dephasing **57**
4.1 Theory 57
4.2 Results 59

5 Conclusion **65**
5.1 Summary 65
5.2 Outlook 66
5.3 Numerics 66
5.4 List of Used symbols 67

A Units and Applied Conventions **69**

B The Selfenergy in Quasi-Particle Approximation **71**

C The Lindhard Polarisation Formula **73**

D The Lindhard Formula for Ideal and Interacting Systems **76**

1 Motivation and General Remarks

The aim of this thesis is a thorough evaluation and analysis of excitonic screening. Screening is the modification of the long-ranged Coulomb interaction between charge carriers and a fundamental example for a many-body problem, as it arises from the interaction of charge carriers in a semiconductor with various surrounding charge carriers. In an excited semiconductor there are electrons, holes and excitons (bound states of electrons and holes), and while the contribution to screening of the former two is well known, excitonic screening has not been investigated much yet. It is however well-known that for low temperatures a large fraction of the electron-hole pairs is bound to excitons, which emphasises the importance of the investigation of excitonic screening. Furthermore the Bose–Einstein-condensation of excitons is one of the current experimental challenges, and since excitonic screening influences the properties of screening the results of this work may help to predict when and under which conditions an excitonic Bose–Einstein-condensation is possible.
Additionally the excitonic contribution to screening influences macroscopic quantities like the susceptibility and the polarisation, i.e. quantities characterising materials. Thus with an improved treatment of screening the results obtained experimentally, can be unterstood better.
The important quantity in the description of screening is the longitudinal polarisation function, and the longitudinal dielectric function respectively. The free carrier polarisation function, also known as random-phase approximation for the polarisation function, was developed by Lindhard [1], and is nowadays one of the standard formulae for the description of screening [2, 3, 4]. The introduction of excitons as new quasiparticles gave reason for various experimentally discovered effects and an expression for the polarisation function of electrons, holes and excitons in a partially ionised plasma was published in [5]. Furthermore in the framework of a theory of a dense exciton gas, where excitons are considered as fundamental particles, the influence of pure excitonic screening on the energy and damping of the excitonic states was investigated in [6]. However a merging analysis of the interplay of screening effects from free carriers and excitons is still missing. This is the aim of this work.
Furthermore this thesis provides a contribution to the analysis of the excitonic linewidth, which can be calculated from the Semiconductor Bloch equations [7], describing the temporal evolution of the macroscopic laser-induced polarisation in optical experiments. One of the quantities causing the decay of the polarisation and the linewidth of the exciton is the diagonal dephasing. Up to now, it was calculated only with a consideration of free carrier screening (see [13, 12] and references therein). It will be shown in this thesis, that excitonic screening can modify the

diagonal dephasing significantly and also that it leads for example to an increased lifetime of the excitons.

Outline

In chapter two the theoretical fundamentals of this thesis will be explained, i.e., the general characteristics of excited semiconductors are presented, a small introduction to Green's function technique is given and the properties of an partially ionised Coulomb plasma in an excited semiconductor are analysed.
In chapter three the polarisation function P, which is a key quantity of this thesis, is evaluated. Firstly the (known) results for free carriers are shown and later the excitonic contribution will be investigated. **The mayor question to be answered is, for which parameters excitonic screening is negligible and for which it is even more important than free carrier screening.**
Since the polarisation function is not directly measureable the results obtained for it are applied to a more concrete physical problem. The macroscopic polarisation, which can be obtained more easily by experiments, depends on the so-called diagonal dephasing, which in turn is a function of the polarisation function. The diagonal dephasing is calculated including the excitonic polarisation function in chapter 4.
In the appendices the excitonic units are explained and some derivation are executed in more detail.

General Method

In many-body physics very often only approximations for physical quantities can be given, reasoned by the enormous complexity of the investigated system and its quantum mechanical character. Often one wants to determine a particular quantity, that is a function of other quantities. However these quantities may in turn depend on the quantity one actually wants to calculate and therefore one is confronted with a problem that has to be solved self-consistently. This can give reason for serious difficulties and therefore a useful method is applied in this thesis: starting with a simple approximation and developing a better one out of it. An example is given in chapter 2 and 3 where chemical potentials are needed to analyse screening, while the chemical potentials in turn are influenced by screening. This problem is not solved selfconsistently here, but a simple approximation is used to obtain the chemical potentials, whatfrom an improved description of screening is developed. This method is in a way comparable to perturbation theory and its acceptance is proven by the obtained results and the comparison with experimental data.

2 Theory

The aim of this chapter is to characterise the basic properties of an excited semiconductor which is subject of all investigation. This is done in section 2.1. Furthermore, the concept of Green's Functions is introduced in 2.3 which are very useful for the analysis of many-body systems and for the correct description of physical properties. Of particular interest are the screened Coulomb potential and the polarisation function, which are the key quantities for the characterisation of screening. For an intuitive access to this topic, a classical introduction to screening will be treated before this (section 2.2). A further characterisation of the investigated system is given in 2.4, taking into account the many-body effects in more detail.

2.1 General Properties of an Excited Semiconductor

Throughout this thesis many-body effects in an excited two-band semiconductor in thermodynamical equilibrium are investigated. A semiconductor consists of electrons and positively charged atom cores. Due to the Coulomb interaction between electrons and cores and because of their quantum mechanical properties an electronic band structure is formed. An introduction to solid state physics is given for example in [8]. An entertaining, but nevertheless detailled guide to semiconductor physics can be also be found in the internet [9].
However, for most optical and electrical properties of semiconductors only two bands are relevant: the valence band v which is the energetically highest completely filled band in an non-excited semiconductor at zero temperature and the conduction band c, which is the lowest lying empty band at zero temperature. It is characteristic for semiconductors that the energy gap E_{Gap} between these bands is in the range of visible light, for typical semiconductors it is $E_{\mathrm{Gap}} \approx 2\,\mathrm{eV}$.
Furthermore, the semiconductor is supposed to be an ideal crystal, i.e., it has no defects and surfaces effects are neglected. Also without importance here are the effects of the lattice beyond the electronic band structure and a dielectric background ϵ_r. Clearly, there is a complicated interaction between electrons and atom cores, however, the atoms and the low lying electrons are treated only as positively charged background, in front of which the electrons exist. Phonon physics is interesting, but it is not in the scope of this thesis.
The band structure of a semiconductor is treated within the effective mass approximation, which means that the valence and the conduction band are supposed to have a parabolic form, leading to effective masses for the valence and conduction

band electrons. An illustration is given in figure (2.1) for ZnSe, were the curvature

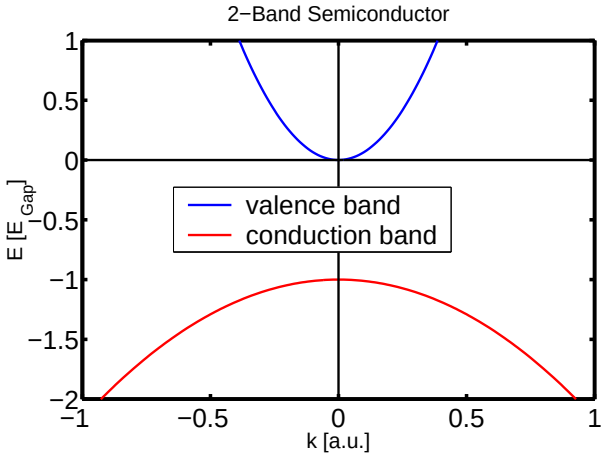

Figure 2.1: model band structure of ZnSe

of the electronic bands is given by the inverse of the effective masses m_c and m_v of the electrons, stated here in terms of the bare electron mass m_0

$$m_c = 0.15 m_0 \quad , \quad m_v = -0.86 m_0 \quad , \quad E_{\mathrm{Gap}} = 2.67\mathrm{eV} \, . \tag{2.1}$$

The energy between these two bands is the gap energy E_{Gap}. As displayed in figure (2.1) ZnSe is a direct semiconductor, i.e. the conduction band minimum lies in momentum space directly above the valence band maximum.
For ideal electrons in thermodynamical equilibrium the occupation of states in momentum space is given by Fermi functions

$$f_\nu(k) = \frac{1}{e^{\beta(E_\nu(k) - \mu_\nu)} + 1} \, , \quad \nu = v, c \, . \tag{2.2}$$

Here, $\beta = 1/k_B T$ is the inverse temperature and $E_\nu(k) = \frac{\hbar^2 k^2}{2 m_\nu}$ is the kinetic energy of the electrons. The chemical potentials μ_ν are determined by the electron density n_ν in the corresponding band ν

$$2 \sum_k f_\nu(k) = n_\nu \, . \tag{2.3}$$

The factor of 2 is due to spin degeneracy and this equation is an equation of state (EoS). It is often useful to change into the electron-hole picture. The description of the electrons in the conduction band remains unchanged while the unoccupied valence band states are treated as independent particles. These are called holes and their properties are related to those of the valence band electrons by

$$m_h = -m_v \quad , \quad e_h = -e_v \quad , \quad f_v(k) = 1 - f_h(k) \tag{2.4}$$

where v is the index for the properties of the electrons in the valence band and h the index for the holes. Their chemical potentials can be obtained like the electron potentials from the EoS (2.3). Changing into this electron-hole picture avoids negative masses for the valence band electrons and the necessity to differentiate between two bands, because if something is said about electrons, now only the electrons in the conduction band are meant. Furthermore, it allows to describe bound states that occur due to the attractive Coulomb interaction between them electrons and holes in analogy to the well-known hydrogen problem (see below). The bound states are called excitons and treated on the same level as non-bound electrons and holes, with their chemical potential being the sum of the chemical potentials of their constituents. That means that they are treated as particles which will be described in section 2.4.1 and is referred to as "chemical picture".
The two-particle Schrödinger Equation for the relative motion of an electron and a hole in a Coulomb potential is known as the Wannier equation

$$-\left[\frac{\hbar^2\Delta_r}{2\mu}+V(r)\right]\psi(r)=E\psi(r) \tag{2.5}$$

which is similar to the Schrödinger equation for the well-known hydrogen problem, except that the reduced mass μ has to be calculated from the electron and hole mass and that the Coulomb potential $V(r)$ contains a dielectric background in this case. Consequently the energy levels are given by

$$E_n=-\frac{E_x^b}{n^2} \tag{2.6}$$

where E_x^b is the binding energy of the ground state exciton, i.e. the excitonic Rydberg. In semiconductors the dielectric background ϵ_r is stronger and the relevant masses are smaller than in hydrogen leading to a much smaller binding energy and a larger Bohr radius,

$$E_x^b = \frac{e^4\mu}{2(4\pi\epsilon_0\epsilon_r\hbar)^2}=0.0224\text{eV}\ll 13.6\text{eV}=\text{Ryd} \tag{2.7}$$

$$a_x = \frac{\hbar^2 4\pi\epsilon_0\epsilon_r}{e^2\mu}=3.648\cdot 10^{-9}\text{m}\gg 5.292\cdot 10^{-11}\text{m}\,. \tag{2.8}$$

Clearly, the binding energy and the excitonic Bohr radius are distinct values for every type of semiconductor. Throughout this thesis will be dealt with ZnSe. While for the optical properties of semiconductors interband processes (e.g. the laser-induced excitation of a valence band electron into the conduction band, leaving a hole behind) are of mayor importance, intraband interactions (e.g. electron-electron scattering within one band) are the reason for screening. But before the effect of screening in a semiconductor and the influence of excitons on this is explained on a quantum statistical level, the general idea of screening and the important physical quantities will be introduced in a classical treatment.

2.2 Classical Theory of Screening

The aim of this chapter is to present the basic ideas and consequences of screening. Screening is a typical many-body effect, as it is the consequence of the interaction of each charge carrier with numerous surrounding charge carriers.
The modification of an external potential by the charge carriers within the excited semiconductors leads to the introduction of a screened potential V^s. This screened potential can be given in terms of the polarisation function P, whose determination is the key point of this thesis.

The properties of an electron-hole plasma are determined by the long range Coulomb interaction. Due to this long range character a charged particle within the plasma does not only interact with a few number of neighboring particles but with a large number of surrounding particles. This leads to a collective behaviour of the charged particles which in turn is responsible for the screening in a Coulomb plasma.
This can be understood by the following considerations. If one brings an externally controlled test charge ρ_{ext} into a plasma it interacts with the surrounding particles causing an induced charge density ρ_{ind}. The external potential Φ_{ext}, the induced potential Φ_{ind} and the effective one, which is the sum of the former two, obey Poisson's equation

$$\Delta\Phi_{\text{ext}}(r,t) = -\frac{1}{\epsilon_0}\rho_{\text{ext}}(r,t)\,, \tag{2.9}$$

$$\Delta\Phi_{\text{ind}}(r,t) = -\frac{1}{\epsilon_0}\rho_{\text{ind}}(r,t)\,, \tag{2.10}$$

$$\Phi_{\text{eff}}(r,t) = \Phi_{\text{ext}}(r,t) + \Phi_{\text{ind}}(r,t)\,, \tag{2.11}$$

or, after Fourier transform in space and time,

$$\Phi_{\text{ext}}(k,\omega) = \frac{1}{k^2\epsilon_0}\rho_{\text{ext}}(k,\omega)\,, \tag{2.12}$$

$$\Phi_{\text{ind}}(k,\omega) = \frac{1}{k^2\epsilon_0}\rho_{\text{ind}}(k,\omega)\,, \tag{2.13}$$

$$\Phi_{\text{eff}}(k,\omega) = \Phi_{\text{ext}}(k,\omega) + \Phi_{\text{ind}}(k,\omega)\,. \tag{2.14}$$

One can see from these equations that the effective potential is determined by the (unknown) induced charge density $\rho_{\text{ind}}(k,\omega)$. The basic idea of a linear theory is that this induced charge density is proportional to the potential causing it,

$$\rho_{\text{ind}}(k,\omega) \propto \Phi_{\text{eff}}(k,\omega)\,. \tag{2.15}$$

One may be confused, that not only the test potential induces the charge density but this problem has to be solved self-consistently: the test field causes the surrounding carriers to rearrange, resulting in an induced charge density. However, the

surrounding charge carriers do actually not experience the bare test potential but a modified one which is the superposition of the test field and the induced field. Thus, the induced charge density is proportional to the effective potential.
The factor of proportionality (multiplied by e^2 for dimension), describing the linear response of the charge density of the system to the effective field is called *polarisation function* P and is one of the key quantities of this thesis. It contains contributions of each particle type in the system, i.e., in an excited semiconductor for example, an electron part and a hole part. Using

$$\Phi_{\text{ind}}(k,\omega) = \frac{1}{k^2\epsilon_0}\rho_{\text{ind}}(k,\omega) = V_k P(k,\omega)\Phi_{\text{eff}}(k,\omega)\,, \tag{2.16}$$

where the fourier transform of the bare Coulomb potential $V_k = \frac{e^2}{k^2\epsilon_0}$ is introduced, and (2.14), one obtains a new expression for the effective potential

$$\Phi_{\text{eff}}(k,\omega) = \frac{\Phi_{\text{ext}}(k,\omega)}{1 - V_k P(k,\omega)}\,. \tag{2.17}$$

Introducing the screened Coulomb potential V^s this can be rewritten as

$$\Phi_{\text{eff}}(k,\omega)\cdot e = V^s(k,\omega) = \frac{e\Phi_{\text{ext}}}{1 - V_k P(k,\omega)}\,. \tag{2.18}$$

As every electron and hole in a semiconductor can be regarded as test charge, whose potential is a bare Coulomb potential one finally obtains

$$V^s(k,\omega) = \frac{V_k}{1 - V_k P(k,\omega)} = \frac{V_k}{\epsilon(k,\omega)}\,. \tag{2.19}$$

where the dielectric function $\epsilon(k,\omega)$ in equation (2.19) describes the modification of the bare Coulomb potential in a medium. A systematic treatment of the polarisation and the dielectric function will be given in the next section, however, to get an idea about it, the static limit $\omega = 0$ of the dielectric function will be examined here. It is well known (see for comparison [10]) that in this limit the dielectric function and the polarisation function are given by

$$\lim_{k\to 0}\epsilon(k,0) = 1 + \frac{\kappa^2}{k^2} \quad , \quad \lim_{k\to 0} P(k,0) = -\frac{\epsilon_0\kappa^2}{e^2} \tag{2.20}$$

where κ, given by

$$\kappa^2 = \frac{4\pi\sum_c e_c^2}{\epsilon_0}\frac{\partial n}{\partial \mu}\,, \tag{2.21}$$

is denoted as inverse screening length. For the screened potential one obtains

$$V^D(k) = \lim_{k\to 0} V^s(k,0) = \frac{e^2}{\epsilon_0(k^2+\kappa^2)} \tag{2.22}$$

and, after Fourier transformation,

$$V^D(r) = \frac{e^2}{4\pi\epsilon_0 r} e^{-\kappa r} \,. \tag{2.23}$$

This potential is called Debye or Yukawa potential and shows that the long range Coulomb interaction of the test particle is shielded by the surrounding plasma charge carriers. The appearance of κ in the exponent explains the denomination as inverse screening length, as it is the inverse of the distance over which the ratio of screened and unscreened potential goes down to $1/e$. As illustration the bare Coulomb potential and the Debye potential are displayed in figure 2.2.

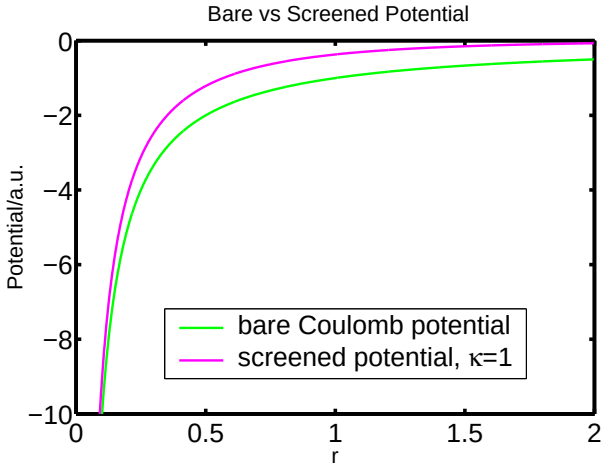

Figure 2.2: comparison of Debye and Coulomb potential in dependence of the distance r

One can see, that the Debye potential goes to zero quite fast, while the Coulomb potential is of long range.

The key result is, that even in this classical treatment the Coulomb interaction is modified or screened by many-body effects. The modification is given by the dielectric or the polarisation function, that are momentum and frequency dependent in general. In chapter three the free carrier polarisation function will be investigated, the static and long-wavelength limit will be reproduced and finally excitonic screening will be considered.

2.3 Many-Body Effects and Green's Functions

In this section a more profound introduction to many-body solid state physics will be given. The arising difficulties will be explained and furthermore Green's functions will be introduced. They are of great help for a well-ordered description of many-body systems. Where possible, well-known and intuitive examples or connections to

results obtained elsewhere are given, to keep the treatment as descriptive as possible.

One characteristic of (elementary) particles is their dispersion relation, i.e. the energy-momentum relation. Massive, noninteracting particles for example are described by

$$E(k) = \frac{\hbar^2 k^2}{2m}$$

while photons are described by

$$E(k) = \hbar k c$$

It is well known in fact that this is not true for interacting particles. In section 2.1 the effective mass approximation was explained. In this approximation electrons and holes are described by a dispersion relation like

$$E^a(k) = \frac{\hbar^2 k^2}{2m_a} \quad \text{with} \quad m_a \neq m_0 \tag{2.24}$$

where m_0 is again the bare electron mass. In general, however, it is not even possible to give such a single-particle relation, i.e., a relation where the energy of a particle is determined only by it's howsoever modified own momentum. The reason is, that the energy of a particle depends on the interaction with *all* other particles, consequently the *single*-particle description is not possible. Because we are investigating a many-body system governed by quantum statistics the interaction can not be calculated exactly, but only in a statistical average.
This problem can be examined systematically and with good success through the introduction of Green's functions. A more detailled introduction to Green's functions is given in [11], and also in [2, 4, 3], here only some necessary basics are stated.

2.3.1 Introduction to Green's Functions

A Keldysh Green's function is defined as

$$G_{a,b}(\underline{1}, \underline{1'}) = -\frac{i}{\hbar}\langle \psi_a(\underline{1})\psi_b^+(\underline{1'})\rangle_C \tag{2.25}$$

where 1 and 1' stand for two different points in space and time: $1 = (r, t)$, $1' = (r', t')$. The spin is neglected throughout this thesis, because no interaction taken into account is spin-dependent, thus the spin causes only spin-degeneracy prefactors. The operators in the brackets are annihilator and creator of a particle of type a and b respectively. The expectation value is time ordered and has to be taken over the double time contour C, this is indicated by the underlines below the times. Of particular interest are

$$G^<_{a,b}(1, 1') = \frac{i}{\hbar}\langle \psi_b^+(1')\psi_a(1)\rangle \text{ and} \tag{2.26}$$

$$G^>_{a,b}(1, 1') = -\frac{i}{\hbar}\langle \psi_a(1)\psi_b^+(1')\rangle\,, \tag{2.27}$$

because for the same time, space and particle type they simplify to the well-known reduced one-particle density matrix

$$G^{<}_{a,a}(1,1') = \frac{i}{\hbar}\rho_a(1)\,, \tag{2.28}$$

$$G^{>}_{a,a}(1,1') = -\frac{i}{\hbar}(1-\rho_a(1))\,. \tag{2.29}$$

The spectral properties of the considered particles are characterised by the retarded Green's function

$$G^{\mathrm{ret}}_{a,b}(1,1') = \Theta(t_1 - t_1')\{G^{>}_{a,b}(1,1') - G^{<}_{a,b}(1,1')\}\,, \tag{2.30}$$

the advanced Green's function

$$G^{\mathrm{av}}_{a,b}(1,1') = -\Theta(t_1' - t_1)\{G^{>}_{a,b}(1,1') - G^{<}_{a,b}(1,1')\}\,, \tag{2.31}$$

and the spectral function

$$\hat{G}_{a,b}(1,1') = G^{>}_{a,b}(1,1') - G^{<}_{a,b}(1,1')\,, \tag{2.32}$$

where $\Theta(t-t')$ is the Heavyside function. When only interband effects are considered, only Green's functions consisting of operators of one type will be of interest, and the index "a,b" can be replaced by "a", standing for electron or hole. Furthermore it is convenient to go into frequency-momentum space, i.e., taking the Fourier transform of the Green's functions, supposing thermodynamical equilibrium and spatial homogeneity.
The Green's function of an interacting particle is given then by Dyson's equation

$$G^{\mathrm{ret}}_{a}(k,\omega) = \frac{1}{\omega - E_a(k) - \Sigma^{\mathrm{ret}}_a(k,\omega)}\,, \tag{2.33}$$

where the selfenergy $\Sigma^{\mathrm{ret}}_a(k,\omega)$ describes the many-body effects in the semiconductor. It is sometimes useful to decompose the selfenergy into a Hartree-Fock part $\Sigma^{\mathrm{HF,ret}}_a(k,\omega)$and a correlation part $\Sigma^{\mathrm{c,ret}}_a(k,\omega)$

$$\Sigma^{\mathrm{ret}}_a(k,\omega) = \Sigma^{\mathrm{HF,ret}}_a(k,\omega) + \Sigma^{\mathrm{c,ret}}_a(k,\omega)\,, \tag{2.34}$$

where the Hartree-Fock contribution represents all many-body effects that can be accounted for in the one-particle description. It is given by

$$\Sigma^{\mathrm{HF,ret}}_a(k,\omega) = -\sum_q V_{k-q} f^a_q \tag{2.35}$$

and frequency independent (see for instance [2]), while the correlation part contains all contributions to the selfenergy that go beyond the Hartree-Fock approximation. In thermodynamical equilibrium the following relations hold

$$G^{<}_{a}(k,\omega) = f^a(\omega)\hat{G}_a(k,\omega)\,, \tag{2.36}$$

$$G^{>}_{a}(k,\omega) = (1-f^a(\omega))\hat{G}_a(k,\omega)\,, \tag{2.37}$$

and the connection between the spectral function $\hat{G}_a(k,\omega)$ and the retarded Green's $G_a^{\mathrm{ret}}(k,\omega)$ function is given by

$$\hat{G}_a(k,\omega) = -2\mathrm{Im}G_a^{\mathrm{ret}}(k,\omega)\,, \tag{2.38}$$

where $\mathrm{Im}G_a^{\mathrm{ret}}(k,\omega)$ stands for the imaginary part of the retarded Green's function. In the following the real part of a function will be labeled by "Re". As the selfenergy represents the many body effects it vanishes for ideal particles, thus the Green's function of non-interacting particles G_0 is given by

$$G_{0,a}^{\mathrm{ret}}(k,\omega) = \frac{1}{\omega - E(k) + i\delta}\,. \tag{2.39}$$

The infinitesimal small damping δ guarantees the causal correctness of the free particle Green's function. By using (2.38) the spectral function of ideal particles is obtained

$$\begin{aligned} \hat{G}_{0,a}(k,\omega) &= -2\mathrm{Im}G^{\mathrm{ret}}(k,\omega) && (2.40)\\ &= 2\pi\delta\left(\omega - \frac{\hbar^2k^2}{2m_a}\right)\,. && (2.41) \end{aligned}$$

Since the spectral function describes the distribution of particle energies the last equation means, that every particle must have an energy of
$\omega = E(k) = \frac{\hbar^2k^2}{2m_a}$. This is the dispersion relation for free particles which was already stated above, and this example shows how properties of the system can be obtained by using Green's functions.
The Green's function of an interacting particle is given by (2.33), the corresponding spectral function is

$$\hat{G}_a(k,\omega) = \frac{-2\mathrm{Im}\Sigma_a^{\mathrm{ret}}(k,\omega)}{(\omega - E_a(k) - \mathrm{Re}\Sigma_a^{\mathrm{ret}}(k,\omega))^2 + (\mathrm{Im}\Sigma_a^{\mathrm{ret}}(k,\omega))^2}\,. \tag{2.42}$$

In general this is an arbitrary function of two variables, and even in the quasi-particle approximation (see below) the spetral function is a Lorentzian, where the real part of the selfenergy causes a shift of the maximum and the imaginary part determines the width of it. This means, that the particle energies are not fixed but statistically distributed over a certain energy range, therefore one can not give a dispersion relation similar to that of free particles.
To obtain the Green's function of electrons or holes in the plasma the selfenergy is needed (2.33). While the Hartree-fock part is known (2.35) the correlation part of the selfenergy is given in the so-called linear V^s approximation by

$$\begin{aligned} \Sigma_a^{c,\gtrless}(k,\omega) &= \sum_q \int \frac{d\omega'}{2\pi} G_a^{\gtrless}(k-q,\omega-\omega')V^{s,\gtrless}(q,\omega')\,, && (2.43)\\ \Sigma_a^{\mathrm{c,ret}}(k,\omega) &= \int \frac{d\omega'}{2\pi}\frac{\Sigma_a^{c,>}(k,\omega) - \Sigma_a^{c,<}(k,\omega)}{\omega - \omega' + i\delta}\,. && (2.44) \end{aligned}$$

The linear V^s approximation is the first term of an expansion of the selfenergy with respect to screened Coulomb potential. For the screened potential hold similar relations as for the Green's functions,

$$V^{s,>} = (1+n(\omega))\hat{V^s} \quad \text{and} \quad V^{s,<} = n(\omega)\hat{V^s}\,, \tag{2.45}$$

$$\hat{V^s} = -2\mathrm{Im}V^{\mathrm{s,ret}}\,, \tag{2.46}$$

$$\text{with} \quad n(\omega) = \frac{1}{e^{\beta\omega}-1}\,. \tag{2.47}$$

This means, that the greater and smaller components of the screened potential can be given by the longitudinal dielectric function

$$V^{s,>}(q,\omega) = -2(1+n(\omega))\,V_q\mathrm{Im}\epsilon^{-1}(q,\omega)\,, \tag{2.48}$$

$$V^{s,<}(q,\omega) = -2n(\omega)\,V_q\mathrm{Im}\epsilon^{-1}(q,\omega)\,. \tag{2.49}$$

$$\tag{2.50}$$

The dielectric function is connected to the polarisation function as described in the classical treatment (2.19)

$$\epsilon(q,\omega) = 1 - V_q P^{\mathrm{ret}}(q,\omega)\,, \tag{2.51}$$

which means that for the retarded screened potential the analogue relation applies as in the classical derivation:

$$V^{\mathrm{s,ret}} = \frac{V_k}{1 - V_k P^{\mathrm{ret}}(q,\omega)}\,. \tag{2.52}$$

Thus, the relations between the screened potential, the dielectric and the polarisation function are the same as that given in the classical treatment. The key quantity is the polarisation function P and it has to be obtained on quantum statistical level to get results. This will be done in chapter 3 with the help of Green's functions.

It can be seen that equations (2.33) and (2.43) form a set of coupled equations, which can be solved only iteratively. Actually this is no surprise, because the whole-many body problem is contained in these equations, so simple analytical solutions could clearly not represent the whole problem. It is however well known from the experiment, that, for low densities, the spectral function of electrons and holes is sharply peaked at a certain energy value $\varepsilon_a(k)$, i.e., it looks like a broadened $\delta-$ function with damping $\Gamma_a(k)$.

$$\varepsilon_a(k) = E_a(k) + \mathrm{Re}\Sigma_a^{\mathrm{ret}}(k,\varepsilon_a) \quad \Gamma_a(k) = -2\mathrm{Im}\Sigma_a^{\mathrm{ret}}(k,\varepsilon_a)\,. \tag{2.53}$$

Using the quasiparticle approximation the selfenergy is taken only at this certain value, giving a new equation for the Green's function

$$G_a^{\mathrm{ret}}(k,\omega) = \frac{1}{\omega - \varepsilon_a(k) + i\Gamma_a(k)/2} \tag{2.54}$$

This approximation is called quasiparticle approximation because the particles type a described by this equation are treated as particles with a dispersion relation similar to that of free particles but shifted by the real part of the selfenergy and with a finite lifetime only, determined by the imaginary part of the selfenergy.
Inserting the quasiparticle approximation into (2.43) a new, managable expression for the correlation part of the self energy can be obtained, for a derivation see Appendix B,

$$\Sigma_a^{\mathrm{c,ret}}(k, \varepsilon_a(k)) = \sum_q \int \frac{d\omega}{2\pi} \frac{[1 - f_q^a] V_{k-q}^{s,>}(\omega) - f_q^a V_{k-q}^{s,<}(\omega)}{\varepsilon^a(k) - \varepsilon^a(q) - \omega - i\Gamma_a(k)/2} \,. \tag{2.55}$$

This equation for the selfenergy in quasiparticle approximation is needed for the calculation of the interband selfenergy, which will be investigated in chapter 4.

2.3.2 Semiconductor Bloch Equations

A characteristic quantity in optical experiments is the susceptibility χ which can be obtained by reflection and transmission measurements. It is connected to the macroscopic polarisation of a system $P'(t)$ by

$$P'(t) = \int_{-\infty}^{t} dt' \chi(t - t') E(t') \,, \tag{2.56}$$

where the upper limit "t" assures the causal correctness. The linear regime between the electric field $E(t)$ of the laser and the polarisation $P'(t)$, also called "linear response" of the medium, is guaranteed only for weak pulses. With Green's function technique an equation of motion for the polarisation (Semiconductor-Bloch equation [7]) can be derived. It turns out, that the polarisation is related to the polarisation function via the so-called diagonal dephasing and consequently, the results of an improved polarisation function will influence the polarisation. Although no complete derivation of the semiconductor Blochequations is given here (but for example [2][2]), the aim of this section is to explain all relevant quantities and to establish the link between the microscopic polarisation function P, whose analysis is the focus of chapter 3 and the diagonal dephasing $\Gamma_a(k, \omega)$ that will be calculated in chapter 4.

Starting again from the general (inter-and intraband) Green's function given by (2.25) one can establish an equation of motion for the Green's function. Applying the limit of equal times on the Keldysh Green's function, it evolves into the 2-band density matrix $f_{ab,k}(t)$which only depends on one time:

$$f_{ab,k}^{\gtrless}(t) = \pm i\hbar \lim_{t' \to t} G_{ab,k}^{\gtrless}(t, t') \quad = \quad \begin{cases} \left.\begin{matrix} (1 - f_k^a(t) \\ f_k^a(t) \end{matrix}\right\} & , a = b = (e, h) \\ \mp p_k(t) & , a = e, b = h \\ \mp p_k^*(t) & , a = h, b = e \end{cases} \tag{2.57}$$

[2] chapter 12

The diagonal elements characterise charge carrier distributions $f_{a,k}(t) = f^a(k,t) = \rho_a(k,t)$, while the off-diagonal elements describe the polarisation, that is induced for example by a laser. The macroscopic polarisation P' is the sum of all polarisation elements $P'(t) = \sum_k p_k(t)$. The equation of motion for the density matrix leads to the well-known Semiconductor-Bloch equations, that can be written as:

$$\begin{aligned} \left[i\hbar\frac{d}{dt} - \varepsilon^{HF}_{a,k}(t) - \varepsilon^{HF}_{b,k}(t) \right] f_{ab,k}(t) & \\ + \sum_c \left[\Omega_{ac,k}(t) f_{cb,k}(t) - f_{ac,k}(t)\Omega_{cb,k}(t) \right] &= I_{ab,k}(t)\,, \end{aligned} \tag{2.58}$$

or, after decomposition into the diagonal elements $f_{a,k}(t)$ and the off-diagonal elements and changing into the electron-hole picture, as

$$\frac{d}{dt} f^a_k(t) + 2\mathrm{Im}\left[\Omega_k(t) p^*_k(t)\right] = I_{aa,k}(t)\,, \tag{2.59}$$

$$\begin{aligned} \left[-i\frac{d}{dt} - E_{\mathrm{Gap}} - \frac{\hbar^2 k^2}{2\mu} - \Delta^{\mathrm{HF}}_k(t) \right] p_k(t) & \\ + \left[1 - f^e_k(t) - f^h_k(t)\right] \Omega_k(t) &= I_{eh,k}(t)\,, \end{aligned} \tag{2.60}$$

where the band indices where omitted for interband quantities, i.e. $\Omega_{eh,k}(t) \to \Omega_k(t)$, $p_{eh,k}(t) \to p_k(t)$.
$\varepsilon^{HF}_{a,k}(t) + \varepsilon^{HF}_{b,k} = E_{\mathrm{Gap}} + \frac{\hbar^2 k^2}{2\mu} + \Delta^{\mathrm{HF}}_k$ is the sum of kinetic and Coulomb-Hartree-Fock energy of the charge carriers. The Hartree-Fock shift of electrons and holes is given by (2.35) and

$$\Omega_k(t) = \left[dE(t) + \sum_q V_{k-q} p_q(t) \right] \tag{2.61}$$

is the Coulomb-Hartree-Fock renormalised Rabi-energy of the laser pulse, i.e. a measure for the coupling power of laser and semiconductor. It is given by the product of the electric field of the laser and the dipole element d and renormalised by Hartree-Fock effects. The left hand side of both equations is given by a collision integral, which contains all the many-body effects beyond the Hartree-Fock approximation. The equation of motion for the polarisation p_k and the carrier distributions $f^a_k(t)$ are coupled to each other. Since the recombination time of electrons and holes, i.e. the life time of the excitons is about $\approx 10^{-9}$s, and thus much larger than the relaxation time of the charge carriers in the semiconductor (10^{-12}s $-$ 10^{-13}s), electrons and holes can assumed to be in quasi-equilibrium, i.e. $f_{a,k}(t) = f_{a,k}$. Thus, only the equation of motion for the polarisation remains. It can be Fourier transformed with respect to t to

$$\left[\omega - \frac{\hbar^2 k^2}{2\mu} - \Delta^{\mathrm{HF}}_k + i\gamma_0(\omega) \right] p_k(\omega) + \sum_q N_k V_{k-q} - N_k dE(\omega) = I_{eh,k}(\omega)\,, \tag{2.62}$$

where ω was replaced by $\omega - E_{\mathrm{Gap}}$, what means, that ω is now the energy difference with respect to the band gap energy. Furthermore the Pauli-Blocking-factor $N_k = 1 - f_k^e - f_k^h$ and a background damping $i\gamma_0(\omega)$, which takes for example interaction with phonons into account, are introduced.
The collision integral $I_{eh,k}(\Omega)$ is given in terms of the correlation selfenergy (see [13])

$$\begin{aligned} I_{eh,k}(\omega) = i \int \frac{d\omega}{2\pi}\frac{d\omega'}{2\pi} \quad & \left[\frac{\Sigma^{c,<}_{eh,k}(\omega,\Omega) G^{>}_{hh,k}(\omega') + G^{>}_{eh,k}(\omega,\Omega)\Sigma^{c,<}_{hh,k}(\omega')}{\omega' - \omega + \Omega/2 + i\delta} \right. \\ + \quad & \frac{\Sigma^{c,<}_{ee,k}(\omega) G^{>}_{eh,k}(\omega',\Omega) + G^{>}_{ee,k}(\omega)\Sigma^{c,<}_{eh,k}(\omega',\Omega)}{\omega' - \omega - \Omega/2 + i\delta} \\ - \quad & \left. > \Leftrightarrow < \right] \end{aligned} \tag{2.63}$$

where two types of terms can be identified. Terms with band-diagonal selfenergies and off-diagonal Green's functions (e.g. second term) are proportional to the polarisation $p_k(\omega)$ and describe interaction processes between the charge carriers, while the other terms are proportional to $p_q(\omega)$ and describe interaction between charge carriers and the laser-induced polarisation. Applying the quasiparticle approximation on the Green's functions (2.54) and the selfenergies in linear V^s approximation (2.55), the collision integral can be summarised to

$$I_{eh,k}(\omega) = \sum_q \left[\Theta_{q,k}(\Omega) p_k(\Omega) - \Theta_{k,q}(\Omega) p_q(\Omega) \right] , \tag{2.64}$$

where the charge carrier interaction is contained in the interband selfenergy

$$\Sigma^c_k(\Omega) = \sum_q \Theta_{q,k}(\Omega) = \Delta^{\mathrm{sc}}_k - i\Gamma_k(\Omega) = \Sigma^c_{e,k}(\Omega) + \Sigma^c_{h,k}(\Omega) , \tag{2.65}$$

that consists of an electron and a hole contribution (because it contains the band-diagonal selfenergies), and whose real part describes a renormalisation of the interband energy, due to charge carrier interaction (in addition to the Hartree-Fock renormalisation). The imaginary part is the so-called diagonal dephasing and corresponds to a temporal decay of the polarisation, that was induced by the laser.
The polarisation-charge carrier interaction can be summarised in the interaction matrix $\Theta_{k,q}(\Omega)$ where the realpart describes the renormalisation of the Coulomb interaction because of many-body effects and the imaginary part is the so-called off-diagonal dephasing. This can be seen by inserting the expression for the collision integral (2.64) into the Semiconductor-Bloch equation for the polarisation (2.62):

$$\begin{aligned} \left[\omega - \frac{\hbar^2 k^2}{2\mu} - \Delta^{\mathrm{HF}}_k - \Sigma^{\mathrm{c,ret}}_k(\omega) + i\gamma_0(\omega) \right] p_k(\omega) & \\ + \sum_q \left[N_k V_{k-q} + \Theta_{k,q}(\omega) \right] p_q(\omega) \quad &= \quad N_k dE(\omega) . \end{aligned} \tag{2.66}$$

It is one aim of this thesis to investigate the influence of excitonic effects on the diagonal dephasing, i.e. on $\mathrm{Im}\Sigma_k^{\mathrm{c,ret}}(\omega)$. Therefore the imaginary part of the interband selfenergy will be calculated with a polarisation function, that takes into account also excitonic screening. The connection of the interband selfenergy , that can be written like (2.55)and the polarisation function is given by the screened potential (2.19) which can be expressed in terms of the polarisation function.
The influence of an excitonic polarisation function on the macroscopic polarisation is a very complex question and beyond the scope of this thesis, but probably subject of a soon to be submitted paper.

2.3.3 The Debye Approximation for the Selfenergy

The selfenergy is a very relevant quantity in many-body physics. However, not everyone may be too familiar with it and therefore it is the aim of this section to convey an idea about it, by presenting some classical considerations. Besides that, the obtained result is also relevant for this thesis, as it was used as a starting point for regarding the many-body effects in an excited semiconductor.
A simple result for the selfenergy is given by a rigid shift (of the selfenergy) and known as Debye approximation $\Sigma_a^{\mathrm{ret}}(k) = -\Delta E^D$. It can be derived classically (see [10][3]).
In this approximation the self energy is the interaction energy U_{int} of a system of charged particles. In general this is

$$U_{\mathrm{int}} = \frac{1}{2}\sum_a \int \rho_a(r')\Phi(r')dr' \tag{2.67}$$

$$= \frac{1}{2}\sum_a N_a e_a \Phi_{\mathrm{ind}}(r_a, 0) \tag{2.68}$$

because the charged particles are point-like and the potential causing the interaction is the induced potential Φ_{ind} which was assumed to be in (2.16)

$$\Phi_{\mathrm{ind}}(k,\omega) = \frac{e_a^2}{k^2\epsilon_0} P(k,\omega)\Phi_{\mathrm{eff}}(k,\omega)\,. \tag{2.69}$$

Applying the static ($\omega \to 0$) and long wavelength ($q \to 0$) limits of dielectric and polarisation function (see (2.20)

$$P(k,0) = -\frac{\kappa^2\epsilon_0}{e_a^2} \quad , \quad \Phi_{\mathrm{eff}}(k,0) = \frac{e_a}{\epsilon_0(k^2+\kappa^2)} \tag{2.70}$$

[3] chapter 2.5&2.6

and taking the Fourier transform the interaction energy can be calculated

$$\begin{aligned} U_{\text{int}} &= \frac{1}{2}\sum_a N_a e_a \int \frac{d^3k}{(2\pi)^3}\frac{e_a^2}{k^2\epsilon_0}P(k,0)\Phi_{\text{eff}}(k,0) \\ &= -\frac{1}{2}\sum_a N_a e_a \int \frac{d^3k}{(2\pi)^3}\frac{e_a^2}{k^2\epsilon_0}\frac{\kappa^2\epsilon_0}{e_a^2}\frac{e_a}{\epsilon_0(k^2+\kappa^2)} \\ &= -\frac{1}{2}\sum_a N_a \frac{4\pi}{(2\pi)^3}\frac{\kappa^2 e_a^2}{\epsilon_0}\left[\frac{1}{\kappa}\arctan(k^2/\kappa^2)\right]_0^\infty \\ &= -\frac{1}{2}\sum_a N_a \frac{e_a^2}{4\pi\epsilon_0}\kappa \end{aligned} \tag{2.71}$$

The last equation shows that (in this approximation) every particle contributes to the interaction energy with

$$\Delta E^D = -\frac{e^2}{2(4\pi\epsilon_0)}\kappa\,. \tag{2.72}$$

This averaged self-energy or rigid shift of every particle is called Debye shift and used as approximation for the selfenergy shift for particles in an interacting system. In excitonic units the Debye shift is

$$E_x^b = \frac{e^2}{2(4\pi\epsilon_0 a_x)} \tag{2.73}$$

$$\Rightarrow \Delta E^D = -\kappa a_x E_x^b = -\kappa\,. \tag{2.74}$$

This leads to an altered dispersion relation

$$\varepsilon(k) = \frac{\hbar^2k^2}{2m_a} + \text{Re}\Sigma_a \approx \frac{\hbar^2k^2}{2m_a} - \Delta E^D = (\alpha_a k^2 a_x^2 - \kappa a_x)E_x^b \tag{2.75}$$

On the right hand side the result is written in excitonic units. This result for the selfenergy can be obtained quantum mechanically as well, see chapter B4 in [2], where it is denoted as Coulomb-hole selfenergy.
This obtained dispersion relation will be used as a starting point of this thesis, i.e. it will be used to determine for instance the chemical potentials μ_a which are parameters of the polarisation function P. By equation (2.43) an improved result for the self energy will be calculated.

2.4 Ideal and Interacting Coulomb Plasma

After this theoretical considerations the characterisation of the investigated system can be improved. As reference system an ideal electron-hole plasma with an electrostatic background was introduced in section 2.1, while the actually interesting

system is one consisting of interacting electrons and holes. This interaction leads to the appearance of bound states which contribute significantly to screening.

Firstly the properties of an ideal Coulomb gas are given as a reminder. As electrons and holes are Fermi particles their distribution is described by Fermi functions and their chemical potentials μ_a ($a = e, h$) in chemical equilibrium can be obtained from the Equation of State (2.3). For given temperature and particle density of the species a the Equation of state can be solved numerically with root finding and the chemical potentials μ_a are obtained. The particle density is equal to the excitation density determined by the experiment (for example by the power of the exciting laser), i.e.

$$n = n_e = n_h \,. \tag{2.76}$$

This seems to be obvious, however, when bound states are considered in the chemical picture, the excitation or total density is no longer equivalent to the free particle density.

2.4.1 Partially Ionised System: Saha's Equation

Electrons and holes are obviously no ideal particles, but subject to electromagnetic forces. This has dramatic effects: firstly the energy levels of electrons and holes are shifted by the selfenergy (see chapter 2) and secondly bound states between particles of both types can occur, due to the attractive character of the electromagnetic force between them.

Considering now a partially ionised system, i.e., a system with electrons, holes and excitons, new questions arise. Again the total density n is predetermined by the experiment, but as electrons and holes can form excitons the densities of free electrons and holes are unknown values. However, the free electron and hole densities are needed to obtain the chemical potentials, see (2.3). In a charge neutral system the free electron and hole densities are equal and connected to the total density via the degree of ionisation α,

$$n = n_e + n_x \quad , \quad n_e = n_h \quad , \quad n_e = \alpha\, n \,. \tag{2.77}$$

Similar to a normal chemical reaction there is a balance between the formation and the decay of excitons in thermodynamical equilibrium,

$$n_e + n_h \Longleftrightarrow n_x \tag{2.78}$$

the tendency of the reaction depending on temperature T and total density n. This means, that there is a linkage between the degree of ionisation α and the free particle densities. The connection is given by Saha's Equation, which is derived below.
In sense of the chemical picture the excitons are identified as new, bosonic particles,

labelled with "x". They obey a similar equation of state as the electrons and holes:

$$n_x^j = \sum_{s,P} g_P^j = 4 \int_{-\infty}^{\infty} \frac{d^3P}{(2\pi)^3} g^j(P)\,, \tag{2.79}$$

where $g^j(P)$ is a Bose function, given by

$$g^j(P) = \frac{1}{e^{\beta(E_{\mathrm{nP}})-\mu_x^j}} \tag{2.80}$$

and the superscript "j" labels the different types of excitons. The prefactor 4 arises because of the fourfold spin-degeneracy of the excitons. For simplicity, and because they are the most abundant ones, only ground state excitons $n = 1$ are considered here. Their chemical potential is simply the sum of the chemical potential of electrons and holes

$$\mu_x = \mu_e + \mu_h\,, \tag{2.81}$$

the same holds for their mass

$$m_x = m_e + m_h\,, \tag{2.82}$$

and their energy, the sum of kinetic and binding energy is given by (see (2.6))

$$E_{1\mathrm{P}} = \frac{\hbar^2 P^2}{2m_x} - E_x^b\,. \tag{2.83}$$

One can now calculate the ratio of the particle densities,

$$\frac{n_x}{n_e n_h} = \frac{4 \int_{-\infty}^{\infty} \frac{d^3P}{(2\pi)^3} \frac{1}{e^{\beta(E_1(P)-\mu_x)}-1}}{2 \int_{-\infty}^{\infty} \frac{d^3k}{(2\pi)^3} \frac{1}{e^{\beta(E^e(k)-\mu_e)}+1} \cdot 2 \int_{-\infty}^{\infty} \frac{d^3k}{(2\pi)^3} \frac{1}{e^{\beta(E^h(k)-\mu_h)}+1}}\,. \tag{2.84}$$

The dispersion relation of electrons and holes is given here by the Debye approximation (2.73)

$$E^a(k) = \frac{\hbar^2 k^2}{2m_a} - \kappa E_x^b a_x\,, \tag{2.85}$$

while no selfenergy shift is applied for the excitons. The reason for the neglectable selfenergy shift of excitons is found by experiments as well as it can be understood by analysing the Semiconductor-Bloch equations [12, 13].
Furthermore the non-degenerate limit is applied, i.e. the Fermi and Bose functions pass into Boltzmann functions, e.g.

$$\frac{1}{e^{\beta(E^e(k)-\mu_e)}+1} \approx e^{-\beta(E^e(k)-\mu_e)}\,. \tag{2.86}$$

With this simplification the integrals can be evaluated, leading to Saha's equation

$$\frac{n_x}{n_e * n_h} = \frac{1-\alpha}{\alpha^2 * n} = \left\{ \frac{\lambda_e * \lambda_h}{\Lambda_x} \right\}^3 e^{-\beta\epsilon_{1s}} \tag{2.87}$$

$$\text{with } \lambda_a = \sqrt{\frac{2\pi\beta\hbar^2}{m_a}}\,,\ \Lambda_x = \sqrt{\frac{2\pi\beta\hbar^2}{m_x}}\,,$$

$$\epsilon_{1s} = 2\Delta E^D - E_b^x\,. \tag{2.88}$$

λ_a and Λ_x are the thermal wavelength of electrons/holes and excitons, respectively, while $2\Delta E^D = 2\kappa a_x E_x^b$ is the total Debye shift (2.73) for electrons and holes. The key point of Saha's equation is that the degree of ionisation is determined only by the total density and the temperature. κ is the inverse screening length and also only a function of temperature and total density. The definition is given by (2.21), which can (after partial integration and in excitonic units) also be written as

$$\kappa^2 = \sum_a \frac{4}{\pi\alpha_a} \int_0^\infty dk f^a(k)\,, \tag{2.89}$$

$$\kappa^2 = 16\pi\beta\alpha n\,, \tag{2.90}$$

where in the last line the Boltzmann limit was applied and the integral evaluated. The used approximations shall be explained and justified in more detail. Firstly this form of Saha's equation is valid only for non-degenerate systems, thus for small densities. It will be seen later (figure 2.6), that for total densities below $n = 10^{17}/\text{cm}^3$ the degeneracy of the system is not important.
Secondly only ground state excitons are considered. Clearly, excited ones exist as well, but from the estimate (Boltzmann limit)

$$\frac{n_{2s}}{n_{1s}} \approx \frac{g_{2s}}{g_{1s}} e^{-\beta|E_{1s}-E_{2s}|} = e^{-\beta(0.75E_x^b)} \tag{2.91}$$

$$\approx 0.078 \quad \text{at } 77\text{K}\,, \tag{2.92}$$

where g_{1s} is a factor for the degeneracy, one can see that the number of excited excitons is small compared to the number of ground state excitons (see also [10]). On the other hand this shows that one can not trust the numerical results without caution.
The third approximation can be seen from (2.88). Due to screening in the plasma the difference between the 1s exciton energy level (labeled with "x") and the continuum edge (conduction band energy) decreases with increasing density, an illustration is given in figure 2.3. In agreement with the experiment the energy levels of the excitons are kept constant [13], while the energy shift for the electrons and holes is approximated by the Debye shift what again is not too bad for small densities. It can also be seen that only free carriers contribute to screening on this level, because

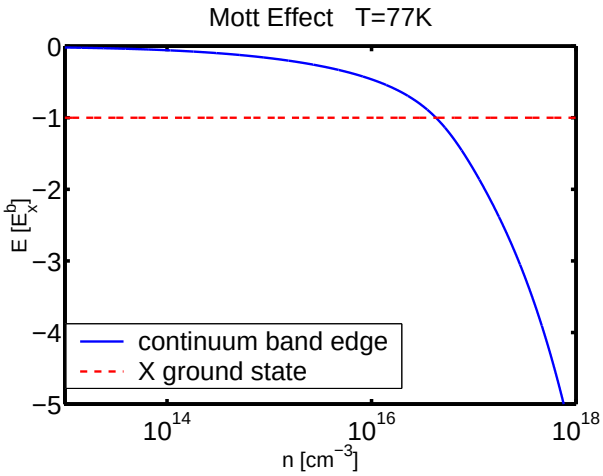

Figure 2.3: continuum band edge and exciton ground state in dependence of the total carrier density n at $T = 20$K

$\kappa^2 \propto \alpha\, n = n_a$. This will be discussed in more detail in chapter 3.

The attentive reader may wonder that screening is treated here on a very simple level, although this thesis deals with screening. The argument explaining this treatment is similar to what was explained in chapter 2 (Approximations for G and Σ). The chemical potentials obtained from Saha's Equation are only parameters in the following calculations of screening, i.e., a simple approximation is used to obtain a better one. This is a fundamental problem in many-body theory but the experience shows that with this concept reasonable results are obtained. It may seem to be a good idea to solve problems selfconsistently, however, experience shows that this often causes more problems than it solves [14].

One can see from (2.88), (2.90) and figure 2.3, that above a certain density the binding energy vanishes and so do the excitons, or better, the occupation of exciton states. This behaviour is referred to as Mott effect. It is connected with a transition from a partially ionised system to a completely ionised system, the so-called called Mott transition.

To be able to calculate the polarisation function the chemical potentials of electrons, holes and excitons have to be known. In the following paragraph is explained how the chemical potentials μ_a, the inverse screening length κ and the degree of ionisation α are calculated.
Saha's equation is used only in the non-degenerate limit and so the chemical poten-

tials will. This simplifies the equation of state used to get the chemical potentials

$$n_a = \sum_{s,k} f_k^a = 2\int_{-\infty}^{\infty} \frac{d^3k}{(2\pi)^3} f^a(k) \;\;,\;\; a = e,h \tag{2.93}$$

For the considered interacting system, the Fermi function is modified by the Debye shift $\Delta E^D = -\kappa a_x E_x^b$ and

$$f^a(k) = \frac{1}{e^{\beta(E_{kin}+\Delta E^D-\mu_a)}+1} \approx e^{-\beta(\alpha_a k^2-\kappa-\mu_a)} \tag{2.94}$$

in excitonic units in the Boltzmann limit. One obtains an analytical expression for the chemical potentials of electrons and holes which is (again in excitonic units)

$$\begin{aligned} n_a &= \sum_{s,k} f(k)^a = 2\int_{-\infty}^{\infty} \frac{d^3k}{(2\pi)^3} \frac{1}{e^{\beta(\alpha_a k^2-\kappa-\mu_a)}} \\ &= \frac{1}{4} e^{\beta\mu_a} e^{\beta\kappa} \left(\frac{1}{\pi\beta\alpha_a}\right)^{3/2} \\ \Rightarrow \mu_a &= \frac{1}{\beta}\ln(4(\pi\beta\alpha_a)^{3/2}\alpha n) - \kappa\,. \end{aligned} \tag{2.95}$$

There are two things to mention: Firstly one must not confuse α which is the degree of ionisation of the system and $\alpha_a = \frac{\mu}{m_a}$ (with μ: reduced mass) which is a mass factor. And secondly, to actually calculate μ_a at given temperature T and total density n one has to know the inverse screening length κ and α. κ is given by

$$\kappa^2 = \sum_a \frac{4}{\pi\alpha_a} \int_0^{\infty} dk \frac{1}{e^{\beta(\alpha_a k^2+\Delta_a-\mu_a)}+1}\,. \tag{2.96}$$

The sum goes over the particle types. To be consistent, the self energy shift is again approximated by the Debye shift. In the non-degenerate limit the integral gives

$$\int_0^{\infty} dk f_a(\alpha_a k^2-\kappa) = \sqrt{\frac{\pi}{4\beta\alpha_a}} e^{\beta\mu_a} e^{\beta\kappa} \tag{2.97}$$

which leads to

$$\kappa^2 = \sqrt{\frac{4}{\pi\beta}} \left\{ \frac{e^{\beta\mu_e}}{(\alpha_e)^{3/2}} + \frac{e^{\beta\mu_h}}{(\alpha_h)^{3/2}} \right\} e^{\beta\kappa}\,. \tag{2.98}$$

Finally, after inserting (2.95) a simple expression for κ is obtained

$$\begin{aligned} \kappa^2 &= \sqrt{\frac{4}{\pi\beta}} \{4(\pi\beta)^{3/2}\alpha n e^{-\beta\kappa} + 4(\pi\beta)^{3/2}\alpha n e^{-\beta\kappa}\} e^{\beta\kappa} \\ \kappa^2 &= 16\pi\beta\alpha n\,. \end{aligned} \tag{2.99}$$

Knowing μ_a in terms of κ and α and κ in terms of α one can now solve Saha's equation to get numerical results. It is transcendent with respect to the total density n (because $\epsilon_{1s} = \epsilon_{1s}(\alpha\, n)$

$$\frac{n_x}{n_e * n_h} = \frac{1-\alpha}{\alpha^2 * n} = \left\{ \frac{\lambda_e * \lambda_h}{\Lambda_x} \right\}^3 e^{-\beta\epsilon_{1s}}\,, \tag{2.100}$$

if one rewrites this equation, however, in terms of the free particle densities n_a it becomes analytical,

$$\begin{aligned} \frac{1-\alpha}{\alpha^2 * n} = \frac{1-\alpha}{\alpha * n_a} &= \left\{ \frac{\lambda_e * \lambda_h}{\Lambda_x} \right\}^3 e^{-\beta\epsilon_{1s}} \\ \Rightarrow \alpha &= \frac{1}{1 + n_a \left\{ \frac{\lambda_e * \lambda_h}{\Lambda_x} \right\}^3 e^{-\beta\epsilon_{1s}}}\,. \end{aligned} \tag{2.101}$$

The binding energy is given by (2.88) and κ is given in terms of n_a by (2.99).
Applying these equations the chemical potentials μ_a, the inverse screening length κ and the degree of ionisation α can be obtained easily.
The Mott effect and the ionisation curves as functions of the total density n are illustrated in figure 2.4. At low densities, the system is fully ionised due to entropy ionisation while with higher densities the occupation of exciton states increases. The minimal degree of ionisation is reached at densities above $10^{16}/\mathrm{cm}^3$ depending on the temperature of the system. On further increase of the density the plasma becomes more and more nonideal, i.e., screening becomes more effective which leads to a lowering of the binding energy of the excitons and finally to the transition back to the fully ionised plasma state.

Another interesting point is that the curves get smoother with higher temperature due to increasing thermal fluctuations. At 20K there is more than one solution for the degree of ionisation for densities near the Mott transition, which would mean that the plasma is in a bistable state with one highly ionised phase and another less ionised phase, while the middle solution is unstable. This effect is subject of controversial discussions, see for instance [16] and [15], current calculations show however that this bistability is unphysical and reasoned by deficiencies of the used model, in particular because of neglecting the interaction between the excitons.
A better treatment of the chemical equilibrium between electrons, holes and excitons would require a better consideration of many body effects via Coulomb- Hartree-Fock and correlation selfenergy [10] (see also chapter 2.3). However the model with Debye shift presented above was a starting point to investigate the influence of bound and free carriers in screening.
Areas in the density-temperature plane where are ambiguous solutions for the degree of ionisation will be avoided therefore the physical properties will be investigated

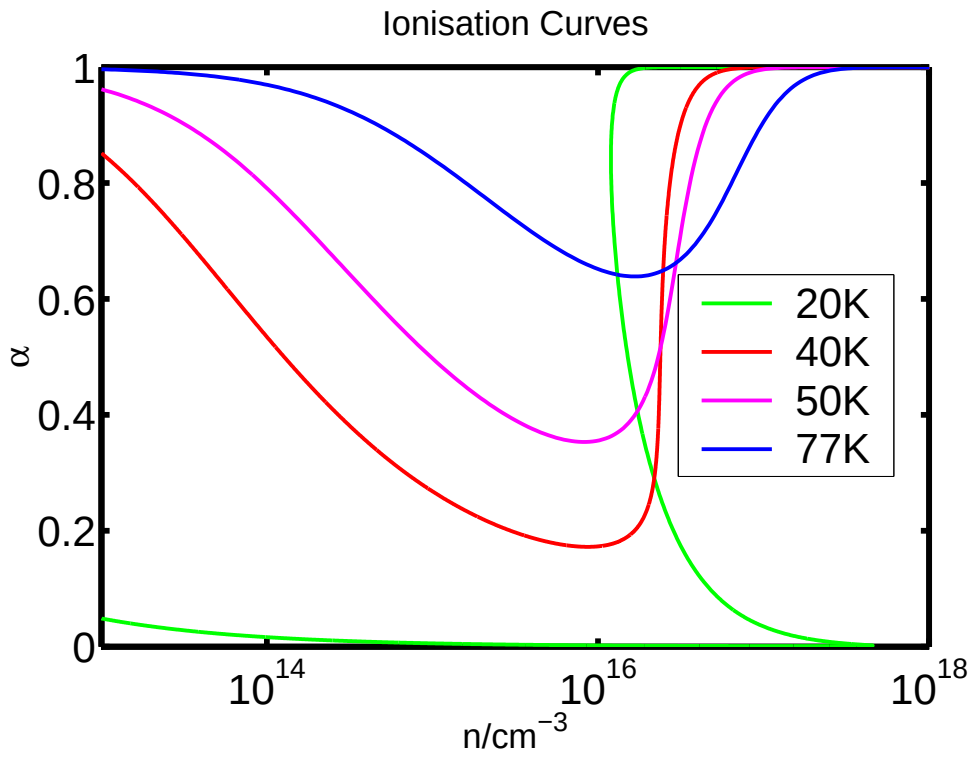

Figure 2.4: degree of ionisation α for 4 temperatures as a function of the total carrier density n

firstly for $T = 77$K, because at this temperature the ionisation curve is unique, smooth and quite close to 1. The second chosen temperature will be $T = 20$K because the corresponding α-curve has a very low minimum. In the focus of this thesis are excitonic contributions to screening, and they become important obviously when the ratio between excitons densities and electron or hole densities is quite large, i.e. for a small value of α.

Finally one can easily calculate the inverse screening length, the degree of ionisation and the chemical potentials of electrons and holes in an interacting, partially ionised system. The exciton chemical potential is simply the sum of the potentials of its constituents, as thermodynamical equilibrium is presumed,

$$\mu_x = \mu_e + \mu_h \,. \tag{2.102}$$

Figure 2.5 shows the chemical potentials of electrons and holes for an interacting plasma calculated with Saha's Equation while for comparison figure 2.6 shows the results for an ideal plasma. Although they show the same physical quantity the pictures do not look similar due to the different physics behind them.
Firstly Saha's equation in the applied form holds for a non-degenerate system and so do the chemical potentials, calculated therewith, while for the ideal system a real

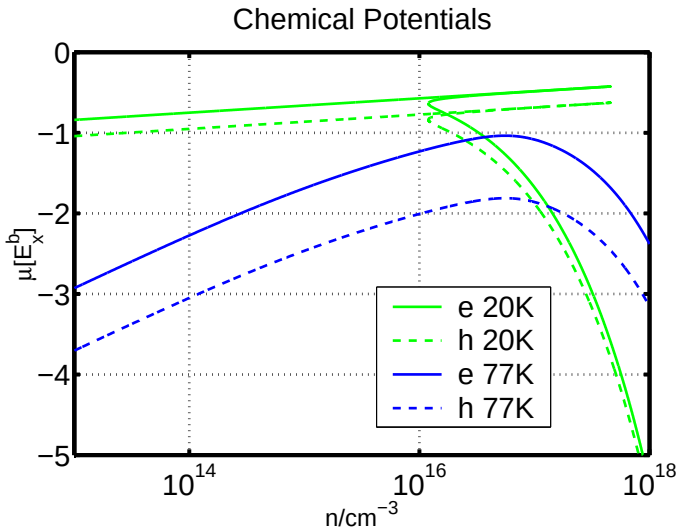

Figure 2.5: chemical potentials for an interacting system $\alpha \neq 1$, for different temperatures in dependence of the total carrier density n

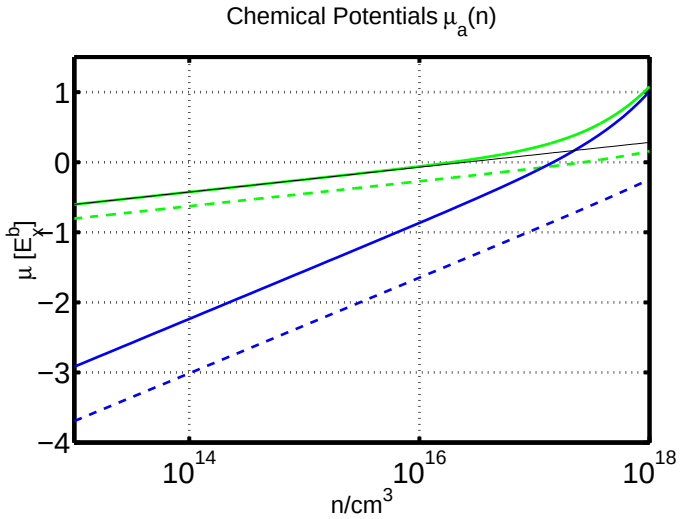

Figure 2.6: chemical potentials for an ideal system $\alpha = 1$, for different temperatures in dependence of the total carrier density (line styles see fig. 2.5 and text)

Fermi function was used (thick lines), see (2.3). The Fermi character leads to a overlogarithmic rise of the potentials at high densities. Because they have a smaller mass, the electrons have higher chemical potentials in general and the degeneracy is more distinct for them. For comparison the thin black line is the chemical potential of an ideal Boltzmann gas at 20K and with the same mass as the electrons, so one can see the influence of the Fermi character: above $n = 10^{17}/\mathrm{cm}^3$ the Boltzmann approximation is no longer valid, especially not for the electrons.

Secondly the chemical potentials calculated with Saha's equation are shifted by the Debye shift (2.95) as a result of the interaction with the surrounding plasma. The Debye Shift increases with $\sqrt{n_a}$ (2.99) and because the chemical potentials (without κ) increase only with $\log(n_a)$ (2.95) the sum of them decreases at high densities. As explained above using the Debye shift for electrons and holes two ionised phases are obtained for $T = 20\text{K}$, resulting in 2 distinct chemical potentials at a given densities for electrons as well as for holes. Again the reason for this is the too simple model for screening applied here.
With the obtained results the polarisation function can be calculated both for an ideal and an interacting system, which is the aim of the next chapter.

3 The Polarisation Function

The crucial quantity for the description of screening is the polarisation function. In this chapter firstly the well-known Lindhard polarisation function will be introduced. It analyses the effect of free carriers on screening. This will be done both for an ideal Coulomb plasma (section 3.1) and an interacting one (section 3.2) which represents the physics of an excited semiconductor much better. Section 3.3 deals with the key point of this thesis: the influence of excitons on screening.

3.1 Polarisation Function of an Ideal Plasma

The polarisation function is the key quantity in the analysis of screening. An ideal electron-hole plasma is the first system where the polarisation function P is calculated for. The results obtained in this section are important for comparison with the results of the interacting system which will be analysed later.

3.1.1 Discussion and Results

The standard formula for the polarisation function of an electron-hole plasma is the Lindhard polarisation function [2, 4, 3]

$$P_1^{\mathrm{ret}}(q,\omega) = 2\sum_{a=e,h}\int \frac{d^3k}{(2\pi)^3}\frac{f^a(k)-f^a(k-q)}{\omega - e^a(k)+e^a(k-q)+i\delta}\,. \qquad (3.1)$$

It describes the dielectric response of an ideal electron-hole plasma due to intraband processes.
Simplified one can say that the Lindhard formula pictures the process of an particle type a going from a state with energy $e^a(k-q)$ and momentum $k-q$ to a state with $e^a(k)$ and momentum k after experiencing the Coulomb potential. The particles transferring the Coulomb interaction in the considered case are plasmons, here with energy ω and momentum q. The Fermi functions describe the occupation of the different states while $\mathrm{Im}P_1^{\mathrm{ret}}(q,\omega)$ can be regarded as the probability for this process to happen. The superscript "et" stands for retarded and means that this polarisation function is the causal right one.
A good illustration of this can be given by means of the Feynman graphs in figure

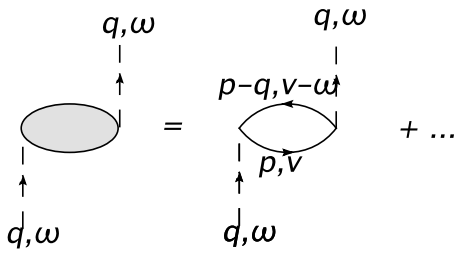

Figure 3.1: Feynman graph for the Lindhard polarisation function (white bubble)

3.1. They are thouroughly explained for example in [4] and [3]. On the left-hand side of the equation is the diagram for the complete and unknown polarisation function (grey bubble), while on the right-hand side the graph for the Lindhard approximation is depicted. Additionally on both sides there is an ingoing and an outgoing line of interaction.
Starting (in the right diagram) from the left bottom end of the diagram and going anticlockwise one can see a plasmon with momentum q and energy ω (dashed line) getting adsorbed by a particle (electron or hole). This particle is therefore shifted into a state with momentum p and energy v. This solid line represents a free one-particle Green's function, the arrow going from left to right (forwards in time) is showing that this state is occupied. Finally the particle emits the plasmon again (right dashed line). The solid line going back to the beginning stands for a non-occupied particle state with momentum $p - q$ and energy $v - \omega$.
In addition to the explanations in chapter 2 a good illustration for screening can be given in Feynman graphs as well, see figure 3.2.

The left diagram in figure 3.2 shows two particles interacting directly via the

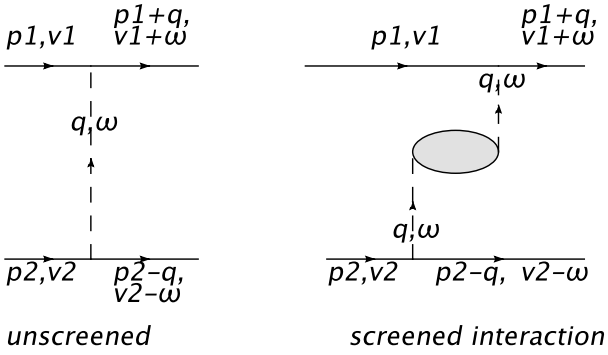

Figure 3.2: illustration for unscreened (left) and first correction to the screened Coulomb interaction (right)

Coulomb interaction, starting with $p1, v1$ and $p2, v2$ and going into other states altered by the transfer momentum and the transfer energy. On the right-hand side however, one can see that this does not happen directly but that there may happen

various processes in between, due to the many-body interactions. The polarisation function (grey bubble) containing infinite numbers of diagrams representing all the possible physical processes. The simplest approximation for the polarisation function is the Lindhard polarisation function, given in Feynman diagrams in figure 3.1 and in a mathematical equation by (3.1).
For a derivation and deeper and more exact explanation see appendix C or [2]. Without any calculation it can already be seen from the equation (3.1) that the polarisation function is small for large momentum transfers q due to the Fermi functions and that it becomes large when the kinetic energy difference in the denominator matches the incoming energy ω.
In the way written down above, equation (3.1) is not manageable for a computer, however, computers are necessary for its evaluation, as it is an integral equation. Firstly the equation has to be decomposed into an imaginary and a real part and secondly the 3-dimensional integration has to be simplified. The decomposition can be done with Dirac's identity

$$\lim_{\delta\to 0}\frac{1}{\omega\pm i\delta}=\frac{P}{\omega}\mp i\pi\delta(\omega)\,, \tag{3.2}$$

where P is the principal value of the integral.
The numerical details are of no interest here so just one remark concerning the implementation: With (3.2) and some appropriate substitutions the imaginary part becomes analytical [3], while the real part is transformed into an effective one dimensional integral which has to be evaluated numerically. The following expressions are obtained (in excitonic units)

$$\begin{aligned}
\mathrm{Im}P_1^{\mathrm{ret}}(q,\omega) &= \frac{1}{8\pi\beta q}\sum_{a=e,h}\frac{1}{\alpha_a^2}\ln\left|\frac{E+e^{-\beta\omega/2}}{E+e^{\beta\omega/2}}\right|\,, &(3.3)\\
\text{with } E &= e^{\beta\left[\frac{\omega^2}{4\alpha_a q^2}+\frac{\alpha_a q^2}{4}-\mu_a\right]}\,,\\
\mathrm{Re}P_1^{\mathrm{ret}}(q,\omega) &= \frac{1}{4\pi^2 q}\sum_a\frac{1}{\alpha_a}\int_{-\infty}^{\infty}dk k f^a(k)\ln\left|\frac{k-\omega_q^-}{k-\omega_q^+}\right|\,, &(3.4)\\
\text{with } \omega_q^{\pm} &= \frac{\omega\pm\alpha_a q^2}{2\alpha_a q}\,.
\end{aligned}$$

Another possibility to calculate the real part from the imaginary part is using a Kramers-Kronig transformation which directly links both parts, however, this is not easier than the executed numerical integration.
In figure 3.3 the results for the real and the imaginary part of the Lindhard polarisation function are displayed. For graphical reasons now and in all forthcoming diagrams always the negative value of the imaginary part will be shown if not stated otherwise. One can see two "hills" in each of the figures. These hills represent the

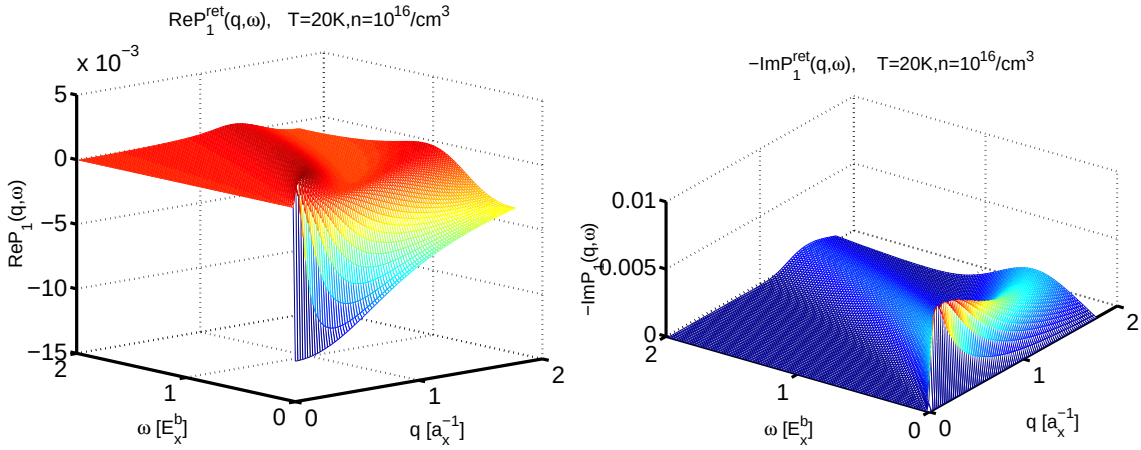

Figure 3.3: real and imaginary part of the polarisation function P_1^{ret} as function of wave vector q and energy ω

poles of the Lindhard function, i.e., the values were

$$\omega = e^a(\mathbf{k}) - e^a(\mathbf{k}-\mathbf{q}) = \hbar^2\left(\frac{\mathbf{kq}}{m} - \frac{q^2}{2m_a}\right) \tag{3.5}$$

can be fulfilled. As a result of the vector character of the momenta this relation is fulfilled not only for a line but for a region. That one recognises not one but two "hills" in every diagram is reasoned by the fact that the polarisation function is the sum of the electron and the hole contributions which have different masses, thus the parabolas have different slopes. Furthermore, one has to consider that the Fermi functions are no Heavyside functions for finite temperature anymore, so there is no sharp border between the regions with and without poles. For a zero temperature discussion see [2], chapter 8.1. The region with poles is called the *continuum of electron-pair excitation*, because it represents the transition of an electron from one state to another as explained above.

3.1.2 Limiting Cases

A very important point for checking the correctness of the numerical results but also for physical interpretation are limiting cases. The most important one is the statical and long wavelength limit, i.e.,

$$\lim_{\omega\to 0, q\to 0, q\neq 0} P_1^{\text{ret}}(q,\omega)\,.$$

It can be shown [2] [1] that the limiting value is

$$\lim_{\omega\to 0,q\to 0,q\neq 0} P_1^{\mathrm{ret}}(q,\omega) = -\sum_a \frac{1}{2\pi^2\alpha_a}\int_0^\infty dk f^a(k) = -\frac{\kappa^2}{8\pi} \tag{3.6}$$

where κ is the inverse screening length (3.6) and excitonic units are used. The limit is real, i.e., the imaginary part of the Lindhard polarisation function vanishes in the static and long wavelength limit. So the classical limit given in chapter 2.2 (there, however, in SI units) is confirmed by this quantum statistically obtained result for the polarisation function. The denomination of κ as inverse screening length is also explained there. Furthermore, the results for the static screened potential and the dielectric function can be approved. The dynamically screened potential is related to the polarisation function via

$$V^{\mathrm{s,ret}}(q,\omega) = \frac{V_q}{\epsilon(q,\omega)} = \frac{V_q}{1-V_qP(q,\omega)}\,. \tag{3.7}$$

The bare Coulomb potential is given in excitonic units by

$$V_q = \frac{8\pi}{q^2}\,. \tag{3.8}$$

For the long wavelength and statical limit one obtains

$$\lim_{\omega\to 0,q\to 0,q\neq 0} \epsilon(q,\omega) = 1+\frac{\kappa^2}{q^2}\,, \tag{3.9}$$

$$\lim_{\omega\to 0,q\to 0,q\neq 0} V^s(q,\omega) = \frac{8\pi}{q^2+\kappa^2} \tag{3.10}$$

and the screened potential is in coordinate representation (after Fourier transformation) and after going back to SI units

$$V^{\mathrm{D}}(r) = \frac{e^2}{4\pi\epsilon_0 r}e^{-\kappa/r} \tag{3.11}$$

the formerly introduced Debye or Yukawa potential.
This limiting value serves also as a test for the numerical results. As κ is given by (3.6) it can be calculated separately from the rest of the polarisation function and serves as a check, whether the limiting value fits to the neighbouring numerical values. Of interest as well are the symmetries of the real and the imaginary part of the dielectric function. In figure 3.4 is shown that the real part is symmetric with respect to ω, while the imaginary part is antisymmetric with respect to it. This can also be obtained from equation (3.3). The antisymmetric behaviour causes the imaginary part of the one-particle polarisation function to vanish for $\omega \to 0$.

[1] chapter 8.3

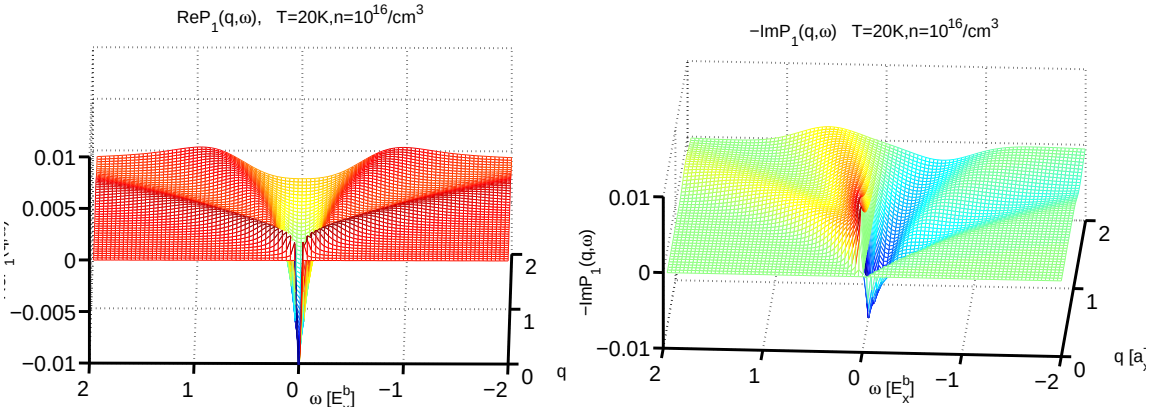

Figure 3.4: the polarisation function P_1 of an ideal coulomb plasma as function of the energy ω and the wave vector q for $T = 20\text{K}$ and $n = 10^{16}/\text{cm}^3$, here also for negative energies to illustrate the symmetry

3.1.3 Plasmons and Plasmon Pole Approximation

The Lindhard formula for the polarisation function or the dielectric function is an integral equation and not too easy to handle. An often used approximation for it is the plasmon pole approximation. It is obtained from

$$\epsilon(q,\omega) = 1 - V_q P_1^{\text{ret}}(q,\omega) \tag{3.12}$$

by considering two limiting cases. Firstly one gets with a Taylor expansion and partial integration

$$\lim_{q\to 0} \epsilon(q,\omega) = 1 - \frac{\omega_{pl}^2}{(\omega + i\delta)^2}\,, \tag{3.13}$$

with the well-known plasma frequency

$$\omega_{pl} = \sqrt{16\pi n_a}\,, \tag{3.14}$$

where ω_{pl} is given in $E_x^b/\hbar$. The second case is the static and long wavelength one, which was already explained above

$$\lim_{\omega\to 0, q\to 0, q\neq 0} \epsilon(q,\omega) = 1 + \frac{\kappa^2}{q^2}\,. \tag{3.15}$$

An interpolation between these limits gives the plasmon pole approximation for the dielectric function

$$\epsilon(q,\omega) = 1 - \frac{\omega_{pl}^2}{(\omega+\delta)^2 - \omega_{pl}^2 \frac{q^2}{\kappa^2}}\,. \tag{3.16}$$

The longitudinal eigenmodes of the plasma, i.e., the frequencies at which the electrons and holes perform collective oscillations are given by the roots of the dielectric

function

$$\epsilon(q,\omega) = 0\,. \tag{3.17}$$

For the Lindhard formula this is equivalent to

$$1 = V_q P_1^{\mathrm{ret}}(q,\omega) \tag{3.18}$$

which has to be solved numerically. For the plasmon pole approximation (3.16) it leads, however, to an analytic dispersion relation

$$\omega_q^2 = \omega_{pl}^2 \left(1 + \frac{q^2}{\kappa^2}\right) \tag{3.19}$$

This quadratic dispersion relation matches particle dispersion relations and so the elementary excitations are identified as quasiparticles and denoted as plasmons.
It is interesting to compare the results for the eigenmodes obtained by using the Lindhard polarisation function with the eigenmodes described by the plasmon pole approximation. The thick blue line in figure 3.5 shows the roots of the plasmon pole

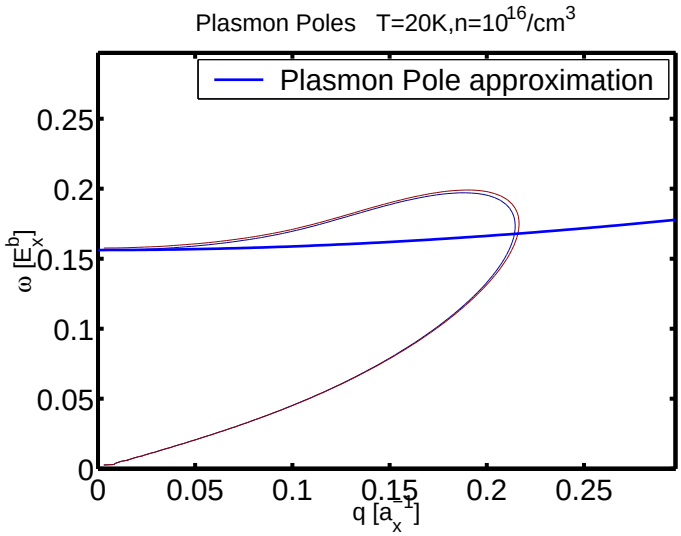

Figure 3.5: eigenmodes of the electron-hole plasma

dielectric function (3.16) while the area between the thin line illustrates the roots of the Lindhard dielectric function (they were obtained graphically here, and the area between the lines is the region where $|1 - V_q P_1^{\mathrm{ret}}(q,\omega)| < 10^{-4}$). One can easily recognise that they start at the same energy ω_{pl}, for other wave vectors, however, the two curves do not match each other. In this approximation the agreement is bad, but the deviation of both curves can be decreased considering a term proportional to q^4.
Nevertheless, the exact analysis of the Lindhard polarisation function demonstrates that the poles are extended only to a finite wavenumber which is not reproduced

by the plasmon pole approximation. It can be seen also that there is an upper and a lower branch of poles. The lower one is not important because in this area of the momentum-energy plain the imaginary part of the polarisation function, i.e. the damping of the plasmons is significant, see figure 3.6 where a contour plot of

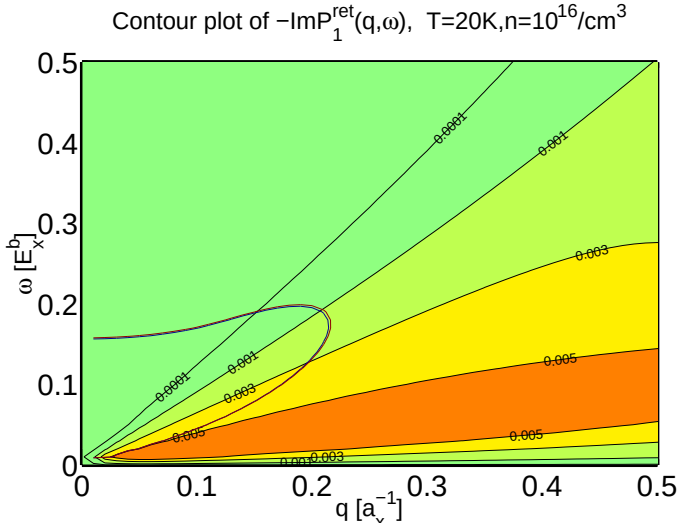

Figure 3.6: contour plot of the imaginary part of the polarisation function P_1 in dependence of wave vector q and energy ω, the red line shows the eigenmodes of the plasma

$\mathrm{Im}P_1(q,\omega)$ is shown. Significant means that the imaginary part is of the order of the real part $\approx 10^{-4}$ which is not fulfilled only for low momentum values of the upper branch.
The plasmon pole approximation may be appropriate for a low level treatment of screening, a system is, however, better characterised by the full Lindhard polarisation function.

3.2 The One-Particle Polarisation Function for a Nonideal Plasma

It is obviously a very crude approximation to neglect the interaction within an electron-hole plasma, so the treatment has to be improved. The influence of the surrounding plasma results in an energy shift of the electrons and holes leading to the dispersion relation

$$e^a(k) \to \varepsilon^a(k) = \alpha_a k^2 + \Delta_a(n,T) = \alpha_a k^2 - \Delta E^D \quad , \; \Delta E^D = \kappa a_x E_x^b \,, \tag{3.20}$$

as explained in chapter 2. The self-energy shift is again approximated by the Debye shift. Furthermore, due to the appearance of excitons the free electron and hole

densities are not equal to the externally controlled total density, but lowered by the degree of ionisation.
The polarisation function $P_1^{\mathrm{ret}}(q,\omega)$ is determined by the chemical potentials of electrons and holes which are in turn functions of the free particle densities. So, when considering a partially ionised system, using the chemical potentials obtained from Saha's equation is the first and intuitive improvement of the Lindhard formula. In fact, in a way this is the first step to consider the influence of excitons on screening! Although they do not contribute to the polarisation function so far, their existence lowers the free charge carrier density, resulting in less effective screening.
With the modified Fermi functions (2.75) and chemical potentials the Lindhard polarisation function (3.1) can be calculated again. For a better distinction the polarisation function of the nonideal system is labeled with the superscript "D", standing for a system where the Debye shift and Saha's equation are taken into account.
The results are displayed in figure 3.7 and they are similar to the graphs in figure

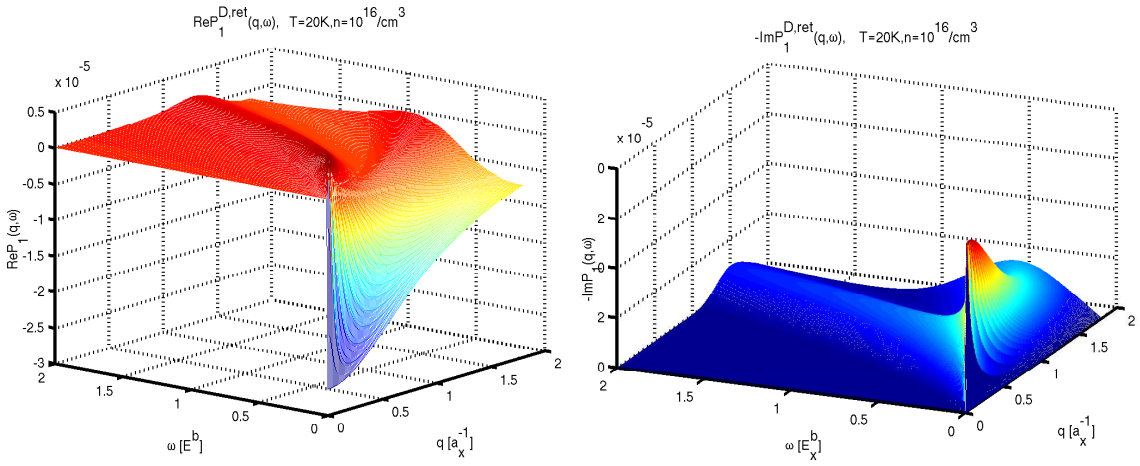

Figure 3.7: real and imaginary part of the polarisation function P_1^D as function of wave vector q and energy ω for a partially ionised plasma

3.3. This is not surprising, because the physical situation behind the graphs is similar as well. In both cases we have a screening electron-hole plasma, in the nonideal system, however, only the fraction α contributes. In fact it can be shown (see appendix D) that in the non-degenerate limit the following relation holds

$$\frac{\mathrm{ReP}_1^{\mathrm{ret,D}}(\mathrm{q},\omega)}{\mathrm{ReP}_1^{\mathrm{ret,0}}(\mathrm{q},\omega)} = \alpha \tag{3.21}$$

where "0" stands for the ideal system and α is the degree of ionisation, defined in (2.77). This means in turn, that the inverse screening length in the interacting plasma is reduced by a factor of α as well. This is logical because with less charge

carriers contributing to screening the *inverse* screening length becomes smaller. It will be shown in the next section, that only the free carriers contribute to statical screening, which justifies the statical screening approximation in Saha's equation where the inverse screening length κ was taken proportional to the degree of ionisation (2.90).
By considering the curves of the degree of ionisation in figure 2.4 the density and temperature combination, which the polarisation function is calculated for, was chosen. At $T = 20\text{K}$ and $n = 10^{16}/\text{cm}^3$ the degree of ionisation is very small ($\alpha \approx 2 \cdot 10^{-3}$) and, therefore, the existing excitons play a significant role. Their contribution to screening will be investigated later, however, to be able to evaluate the importance of excitonic screening one clearly has to know the results of free carrier screening.
As in the ideal system plasmon poles appear as well, but, as the plasma frequency is proportional to the root of the free carrier density (3.14), for much smaller wave vectors and energy values. This is depicted in figure 3.8, while for the considered parameters holds $\sqrt{\alpha} \approx 0.045$).

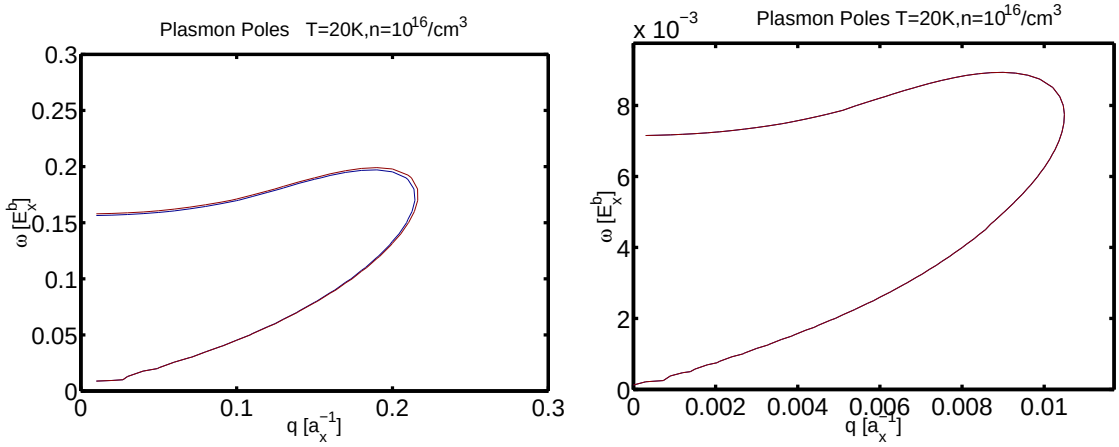

Figure 3.8: plasmon poles in an ideal (left) and an interacting electron hole plasma (right) (the two figures do not have the same scale)

Comparing the results of the polarisation function obtained for the ideal and the interacting plasma the most important result is that the polarisation function in the nonideal plasma is lowered by the degree of ionisation. Consequently in a system with a low degree of ionisation the free carrier contribution to screening becomes less important, while the excitonic contribution becomes significant. The investigation of the excitonic polarisation function will be the aim of the next chapter.

3.3 The Excitonic Polarisation Function

3.3.1 Introduction and Discussion

It was shown in the last section that in an interacting plasma the fraction of bound states can be quite large and that the one-particle polarisation function is quantitatively changed significantly by many-body effects. However, so far excitons were not considered to contribute to screening. As a first approximation this may be sufficient, because they are charge neutral, but for refined results for the dielectric function excitons have to be taken into account.
Talking about excitons one has to be careful because, in analogy to the hydrogen problem, not only bound states exist but also scattering ones. Consequently one also has two parts of the two-particle polarisation function $P_2(q,\omega)$, a fraction from the bound states $P_2^b(q,\omega)$ and a fraction from the scattering $P_2^{sc}(q,\omega)$ states,

$$P_2(q,\omega) = P_2^{\mathrm{b}}(q,\omega) + P_2^{\mathrm{sc}}(q,\omega)\,. \tag{3.22}$$

It will be shown later that the contribution of the scattering electron-hole states to the polarisation function is very small compared to that of the bound states.
The expression of the two-particle polarisation function can be derived with the help of Green's function technique and was published in [5]. It is also explained in [3]. The retarded two-particle polarisation function is given by

$$\begin{aligned}
P_2(q,\omega) &= P_2^b(q,\omega) + P_2^{sc}(q,\omega)\,, \\
P_2^{\mathrm{b,ret}}(q,\omega) &= +4\sum_{n,n'} P_{2,nn'}^{\mathrm{b,ret}}(q,\omega)\,, && (3.23)\\
P_{2,nn'}^{\mathrm{b,ret}}(q,\omega) &= |D_{nn'}|^2 \int \frac{d^3P}{(2\pi)^3}\frac{g_{ab}(E_{nP}^{ab}) - g_{ab}(E_{n'P-q}^{ab})}{\omega - E_{nP}^{ab} + E_{n'P-q}^{ab} + i\delta}\,, && (3.24)\\
P_2^{\mathrm{sc,ret}}(q,\omega) &= -4\sum_{a,b}\int \frac{d^3p_1}{(2\pi)^3}\frac{d^3p_2}{(2\pi)^3} \\
&\quad \frac{g_{ab}(e_{p_1}^a + e_{p_2}^b) - g_{ab}(e_{p_1-q}^a + e_{p_2}^b)}{\omega - e_{p_1}^a + e_{p_1-q}^b + i\delta}\,. && (3.25)
\end{aligned}$$

At first the binding part will be investigated. The expression for it can also be obtained investigating the properties of an excitonic gas, i.e., without free carriers, see [6]. The binding part of the two-particle polarisation function can be decomposed into contributions arising from the different states n and n' of the exciton before and after experiencing the Coulomb interaction. So $P_{2,11}^{\mathrm{b,ret}}(q,\omega)$ is the two-particle contribution to the polarisation function of the excitons that stay in their ground

state. The mathematical expressions of these polarisation function matrix elements are similar to the Lindhard polarisation function (3.1), except for the density correlation factors $D_{nn'}$, which are explained later (3.42), and the one-particle energies $e^a(k)$, which are replaced by the two-particle energies E^{ab}_{nP}. These are defined as

$$E^{ab}_{nP} = \frac{\hbar^2 P^2}{2M} + E_n \,, \tag{3.26}$$

where the first term is the kinetic energy of the centre of mass motion and the second term is the binding energy of the exciton

$$E_n = -\frac{E^b_x}{n^2} \,, \tag{3.27}$$

depending only on the principle quantum number n in analogy to the hydrogen atom. In contrast to the dispersion relations of electrons and holes there is no selfenergy shift considered for the excitons. This shift is found to be negligible as explained in chapter 2.3. Furthermore the Fermi functions describing the occupation of electron or hole states are replaced by Bose functions describing excitons, which are Bose particles, since their total spin is even,

$$g_{ab}(E^{ab}_{nP}) = \frac{1}{e^{\beta(E^{ab}_{nP}-\mu_x)}+1} \quad , \quad \mu_x = \mu_a + \mu_b \,. \tag{3.28}$$

A simplified physical explanation can be given in analogy to that for the Lindhard polarisation function: an exciton (bound state) experiences the Coulomb force and passes from a state with centre-of-mass momentum P and principle quantum number n to a state with $P - q$ and n'. This means, that, for example transitions from a 1s exciton into a 2s exciton are allowed. The value describing the propability for these transitions is the matrix element $|D_{nn'}|^2$ (3.42), which is also called density correlation for reasons explained later. The last thing to mention is the prefactor 4 which is caused by the fourfold spin degeneracy for excitons, in opposition to electrons and holes which are only twofold degenerate in spin.
In Feynman graphs the two-particle polarisation function is given by several diagrams. For illustration one of these is depicted in figure 3.9.

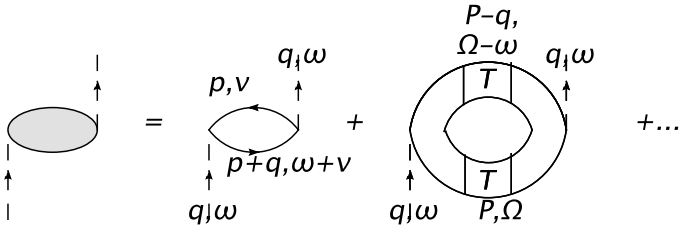

Figure 3.9: Feynman graphs for the excitonic polarisation function (not complete)

It can be seen there, that an electron experiences the Coulomb force, therefore, the two-particle state of electron and hole (the "T" in the diagram, standing for the T-Matrix) is transferred into a state with higher energy Ω and centre-of-mass momentum P while a state with $\Omega - \omega$ and $P - q$ is unoccupied.
To describe bound states a partial summation of infinite orders of interaction is necessary. This is done by the T-matrix which is given in ladder approximation by the iterative equation

$$T = V + V\mathcal{G}T\,, \tag{3.29}$$

or, in Feynman diagrams, by figure 3.10.

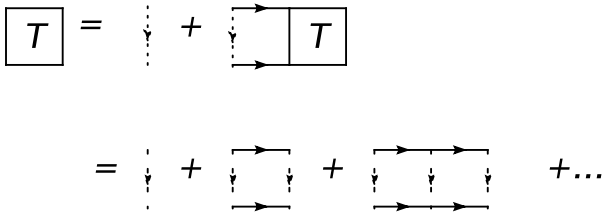

Figure 3.10: Feynman graphs for the T-matrix

V is the bare Coulomb potential, $\mathcal{G}$ is the uncorrelated part of the two-particle Green's function, describing an ideal two-particle state (in analogy to the ideal single-particle Green's function, see chapter 2). Since the T-matrix describes two particle systems, where the constituents are coupled to each other via the Coulomb interaction it is not surprising, that the eigenfunctions of the T-matrix are the hydrogen eigenfunctions. Evaluating the diagrams contributing to the two-particle polarisation function one ,therefore, has to change from a one particle base, which is the appropriate base for single-particle Green's function, into the hydrogen states, where the T-matrix is given in. The transfer from the one-particle states to the two-particle states leads to transfer amplitudes like

$$\langle p_1^a p_2^b | nP \rangle = \psi_n(p_{\mathrm{rel}}^{ab})\,, \tag{3.30}$$

where p_1^a, p_2^b are the single-particle momenta of particles type a and b and P, n are the two-particle quantities centre of mass momentum and principal quantum number, respectively. These transfer amplitudes are the hydrogen eigenfunction (in momentum space) with relative momentum $p_{\mathrm{rel}} = \frac{m_b p_1 - m_a p_2}{m_a + m_b}$ and give rise to the density correlation functions $D_{nn'}$, which influence the binding part of the two-particle polarisation function, see (3.23).
The scattering hydrogen eigenfunctions are known as the confluent hyper-geometric functions and are also a base of two-particle states, however, they are approximated as plane waves here. Plane waves are described by single-particle momenta, therefore, the transfer amplitudes reduce to unity, and nothing like the density correlation functions $D_{nn'}$ appears in the scattering part.

The scattering part of the polarisation function

$$P_2^{\mathrm{sc,ret}}(q,\omega) = -4\sum_{a,b}\int \frac{d^3p_1}{(2\pi)^3}\frac{d^3p_2}{(2\pi)^3}\frac{g_{ab}(e^a_{p_1}+e^b_{p_2})-g_{ab}(e^a_{p_1-q}+e^b_{p_2})}{\omega - e^a_{p_1}+e^b_{p_1-q}+i\delta}\,, \tag{3.31}$$

is the contribution of unbound electron-hole states (two-particle states).
The energies in the denominator e^a_p are single-particle kinetic energies while the Bose functions are

$$g_{ab}(e^a_{p_1}+e^b_{p_2}) = \frac{1}{e^{\beta(e^a_{p_1}+e^b_{p_2}-\mu_a-\mu_b)}-1}\,. \tag{3.32}$$

A difference worth to mention between the single-particle polarisation function and the excitonic polarisation function is the number of internal variables. In the Lindhard formula the initial momentum p of the interacting particle is not determined by external parameters, however, the final momentum is determined by the initial momentum and the momentum transfer q. In the scattering part of the two-particle polarisation function there are the two initial momentums of the electron and the hole that are not fixed, so there are two internal variables or degrees of freedom.
Eventually, for the binding part there are three: the centre-of-mass momentum P, the initial principal quantum number n and the final principal quantum number n'. While there is a conservation law for momenta, establishing a fixed relation between initial and final momentum there is no such law for principal quantum numbers. Thus the initial and the final quantum number are not related to each other, resulting in one additional internal variable. Clearly, to get the contribution of all bound or scattering states to the polarisation function, over all internal variables has to be integrated/summed up.

For numerical evaluation the expressions for the excitonic polarisation function have to be reformulated (splitting into real and imaginary part, execution of the

integration over the angles). The binding part is given by

$$\mathrm{Re}P_2^{\mathrm{b,ret}}(q,\omega) = +4\sum_{n,n'}\mathrm{Re}P_{2,nn'}^{\mathrm{b,ret}}(q,\omega)\frac{1}{8\pi^2\alpha' q}\,, \tag{3.33}$$

$$\mathrm{Re}P_{2,nn'}^{\mathrm{b,ret}}(q,\omega) = |D_{nn'}|^2\int_{-\infty}^{\infty}dP\,P g_{ab}(\alpha' P^2+E_n)\ln\left|\frac{q_{nn'}^{+}+P}{q_{nn'}^{-}+P}\right|\,, \tag{3.34}$$

$$\mathrm{Im}P_2^{\mathrm{b,ret}}(q,\omega) = \sum_{n,n'}\mathrm{Im}P_{2,nn'}^{\mathrm{b,ret}}(q,\omega)\frac{-1}{4\pi\alpha'^2\beta q}\,, \tag{3.35}$$

$$\mathrm{Im}P_{2,nn'}^{\mathrm{b,ret}}(q,\omega) = |D_{nn'}|^2\ln\left|\frac{1-e^{-\beta(\alpha'(q_{nn'}^{+})^2+E_n-\mu_x)}}{1-e^{-\beta(\alpha'(q_{nn'}^{-})^2+E_n-\mu_x)}}\right|\,, \tag{3.36}$$

$$\text{with}\ \ \frac{1}{\alpha'}=\frac{1}{\alpha_e}+\frac{1}{\alpha_h}\quad,\quad q_{nn'}^{\pm}=\frac{\omega\pm(\alpha' q^2-E_n+E_n')}{2\alpha' q}\,, \tag{3.37}$$

$$E_n=-\frac{1}{n^2}\quad,\quad \mu_x=\mu_a+\mu_b\,, \tag{3.38}$$

while the scattering part can be written as

$$\mathrm{Re}P_2^{\mathrm{sc,ret}}(q,\omega) = \frac{1}{4\pi^4 q}\int dp_2\sum_{a,b\,a\neq b}\frac{1}{\alpha_a}\int_{-\infty}^{\infty}dp_1 p_1 \tag{3.39}$$
$$g_{ab}(\alpha_a p_1^2+\alpha_b p_2^2)\ln\left|\frac{q_a^{+}+p_1}{q_a^{-}+p_1}\right|\,,$$

$$\mathrm{Im}P_2^{\mathrm{sc,ret}}(q,\omega) = \frac{-1}{8\pi^3 q\beta}\int dp_2 p_2^2\sum_{a,b}\ln\left|\frac{1-e^{-\beta(\alpha_a(q_a^{+})^2+\alpha_b p_2^2-\mu_x)}}{1-e^{-\beta(\alpha_a(q_a^{-})^2+\alpha_b p_2^2-\mu-x)}}\right|, \tag{3.40}$$

$$\text{with}\ \ q_a^{\pm} = \frac{\omega\pm\alpha_a q^2}{2\alpha_a q}\,, \tag{3.41}$$

where α_a is defined in (A.5). Since the binding part of the two-particle polarisation function and the Lindhard polarisation function (3.3) have a similar structure, they also have the same symmetries: the real part is symmetric with respect to q and ω, while the imaginary part is antisymmetric. Clearly, as an interacting and partially ionised system is investigated, the chemical potentials obtained from Saha's equation have to be used.

Before getting to the results one last remark concerning the density correlation factors $D_{nn'}(q)$, that are given by

$$D_{nn'}(q) = d_{nn'}(\alpha_e q)-d_{nn'}(-\alpha_h q)\,, \tag{3.42}$$

$$d_{nn'}(q) = \int d^3k\psi_n^*(k)\left[\psi_{n'}(k-q)\right] \tag{3.43}$$

where the wavefunctions $\psi_n(k)$ were introduced in (3.30). The density correlation factors are the sum of an electron and a hole contribution, weighted by their charge,

thus effectively a difference. Considering only the electron or hole fraction they would describe the propability amplitude for an exciton to go from state with principal quantum number n to state with n'. The two parts arise because the Coulomb interaction can affect either the electron or the hole, which differ in their masses. For a transfer momentum $q = 0$ there is actually no interaction and thus there is no difference between electrons and holes.
Clearly the 1s and 2s excitons are the most abundant ones, so only their contribution to the polarisation function is computed. For the resulting 4 parts analytical expressions for the density correlation functions $D_{nn'} = d_{nn'}(\alpha_e q) - d_{nn'}(\alpha_h q)$ can be derived. These are given by

$$d_{12}(q) = \frac{4\sqrt{2}q^2}{(q^2+2.25)^3} \quad = \quad d_{21}(q)\,, \tag{3.44}$$

$$d_{11}(q) = \frac{16}{(q^2+4)^2} \quad , \quad d_{22}(q) = \frac{2q^4 - 10q^2}{(q^2+1)^4} \tag{3.45}$$

and are displayed in figure 3.11. The most important effect of these prefactors

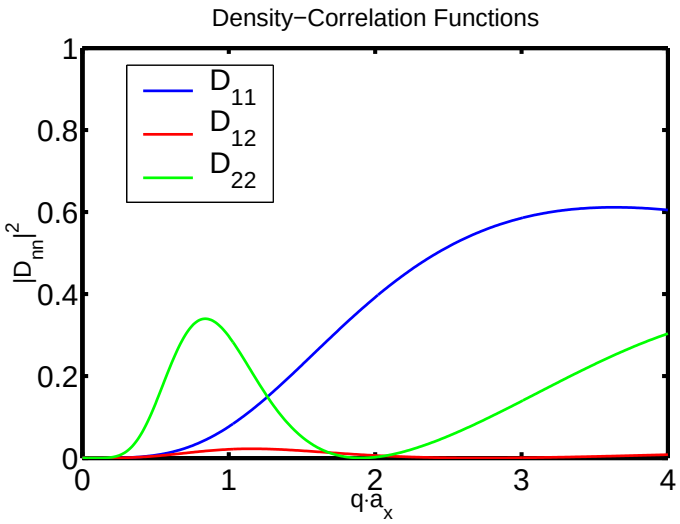

Figure 3.11: density correlation functions $|D_{11}(q)|^2$,$|D_{12}(q)|^2 = |D_{21}(q)|^2$ and $|D_{22}(q)|^2$ as functions of the wave vector q

is, that the static $\omega = 0$ and long wavelength $q \to 0$ limit of the two-particle polarisation function vanishes, i.e., only free carriers contribute to static screening. This is actually the belated justification for the static screening approximation in the derivation of Saha's equation, were only free carriers were taken into account. Furthermore, it can be obtained from figure 3.11 that the off-diagonal elements are much smaller than the diagonal elements, which of course will influence the importance of the two-particle polarisation contributions $P_{nn'}$.
A further result of the density correlation factor is, that no excitonic elementary

excitations were found. These are given by the roots of the dielectric function

$$\epsilon^{\mathrm{ret}}(q,\omega) = 1 - V_q P^{\mathrm{ret}}(q,\omega) \tag{3.46}$$

and are found for the one-particle polarisation function for small wave vector values, because $V_q \propto q^{-2}$. Since the binding part of the two-particle polarisation function is proportional to to $|D_{nn'}|^2$, which vanishes for small wave vectors, there were no roots found for the two-polarisation function. However, it was shown, that for a pure exciton gas at much higher densities there can be excitonic elementary excitations, see [6].

3.3.2 Numerical Results

The next step is to evaluate the results obtained by the excitonic polarisation function. The interesting question is, whether and for which energies and wave vectors the results of the two-particle contribution to the polarisation function are at least of the same order of magnitude as the results for the Lindhard formula. This will show when the influence of excitons on screening becomes important!

Binding Part

At first the influence of ground state excitons on screening will be analysed. In figure 3.12 the results for $P^{\mathrm{b,ret}}_{2,11}(q,\omega)$ are displayed. Similar to the results of the Lindhard

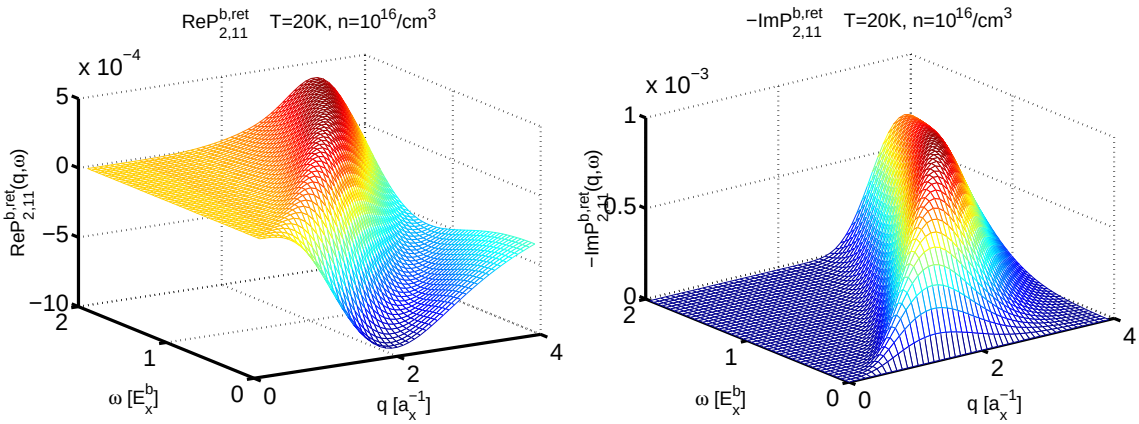

Figure 3.12: real and imaginary part of the binding part of the two-particle polarisation function $P^{\mathrm{b,ret}}_{2,11}(q,\omega)$ as a function of wave vector q and energy ω and for $T = 20\mathrm{K}$ (only ground state excitons considered)

polarisation function in both the real and the imaginary part a "hill" is apparent. This is the continuum of *exciton pair excitations* and since there is only one particle type now (1s excitons) there is also only one continuum, in contrast to the Lindhard polarisation function where there were two "hills", one for electrons and one for

holes. The polarisation function (3.23) becomes large when the denominator is small, i.e., when

$$-E^{ab}_{nP} + E^{ab}_{n'P-q} \approx \omega\,. \tag{3.47}$$

For the considered $P^{\mathrm{b,ret}}_{2,11'}(q,\omega)$ this is (in excitonic units)

$$\begin{aligned} \omega &= -\alpha' P^2 + \frac{1}{n^2} = \alpha'(\mathbf{P}-\mathbf{q})^2 - \frac{1}{n'^2}\,, \\ &= -2\alpha'\mathbf{P}\mathbf{q} + \alpha' q^2\,. \end{aligned} \tag{3.48}$$

The quadratic shape of the exciton pair excitation is clearly visible in figure 3.12. The real and imaginary parts of $P^{\mathrm{b,ret}}_{2,12}(q,\omega)$, $P^{\mathrm{b,ret}}_{2,21}(q,\omega)$ and $P^{\mathrm{b,ret}}_{2,22}(q,\omega)$ are depicted in figures 3.13, 3.14 and 3.15. While $P^{\mathrm{b,ret}}_{2,12}(q,\omega)$ is only one order of magnitude

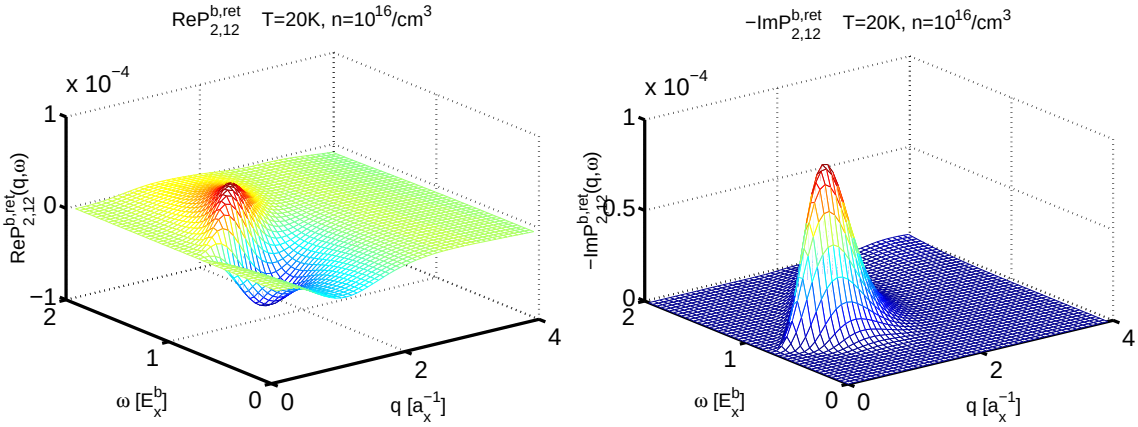

Figure 3.13: real and imaginary of $P^{\mathrm{b,ret}}_{2,12}(q,\omega)$ as a function of wave vector q and energy ω

smaller than $P^{\mathrm{b,ret}}_{2,11}(q,\omega)$, the other two contributions are clearly less important. One reason are the density correlation functions which are much smaller for the off-diagonal elements than for the diagonal ones. More important is, however, the occupation of exciton states. The number of ground state excitons is much bigger than the number of excited ones, therefore, the contribution where a 1s exciton is transfered to a 2s exciton $P^{\mathrm{b,ret}}_{2,12}(q,\omega)$, is much bigger than $P^{\mathrm{b,ret}}_{2,21}(q,\omega)$, which describes the opposite process, simply because the ground states are occupied more often. For the same reason $P^{\mathrm{b,ret}}_{2,22}(q,\omega)$ is much smaller than $P^{\mathrm{b,ret}}_{2,11}(q,\omega)$. This can be estimated by a Boltzmann approximation

$$\frac{n_{2s}}{n_{1s}} \approx \frac{g_{2s}}{g_{1s}} e^{-\frac{|E_{1s}-E_{2s}|}{\beta}} = e^{-\beta(0.75E^b_x)}\,, \tag{3.49}$$

$$\approx 6.3\cdot 10^{-5} \quad \text{at T} = 20\text{K}\,, \tag{3.50}$$

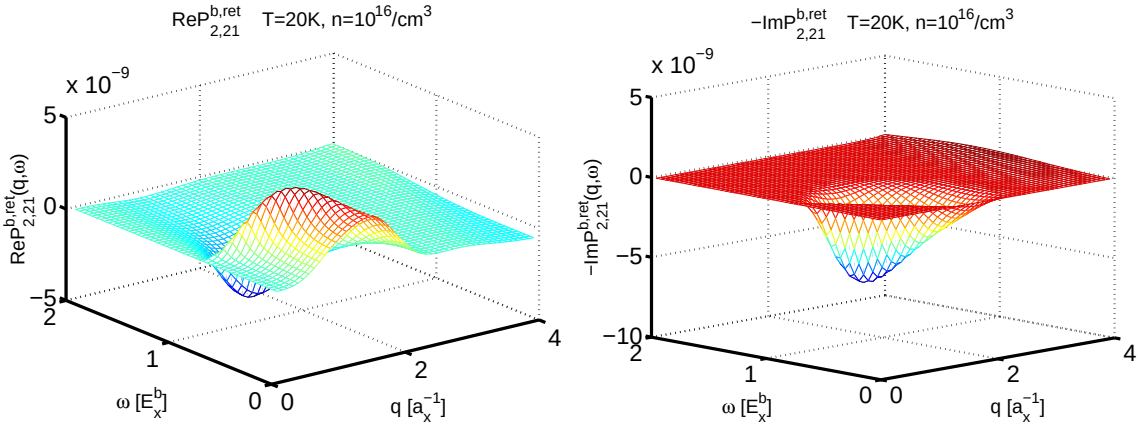

Figure 3.14: real and imaginary part of $P^{\mathrm{b,ret}}_{2,21}(q,\omega)$ as a function of wave vector q and energy ω

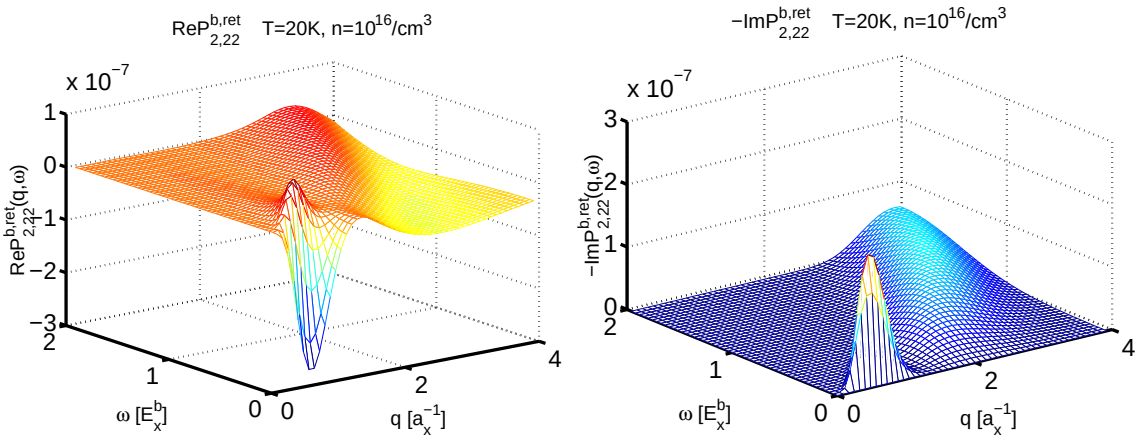

Figure 3.15: real and imaginary part of $P^{\mathrm{b,ret}}_{2,22}(q,\omega)$ as a function of wave vector q and energy ω

where g_n is the degeneracy of states.
It can also be seen that the continuum of exciton pair excitations is shifted in the off-diagonal contributions by $\approx 0.75E^b_x$ because the transition of the exciton from the ground state to the first excited state requires an energy transfer of $\omega = 0.75E^b_x$, while the opposite process allocates this energy. Perhaps surprising is, that in figure 3.14 the imaginary part of the polarisation function is positive in contrast to all other contributions. Since the dielectric function is given by

$$\epsilon(q,\omega) = 1 - V_q P(q,\omega) \tag{3.51}$$

this corresponds to a contribution to the dielectric function with negative damping, i.e., the causality is violated. However, throughout the thesis an excited semiconductor in thermodynamical equilibrium is considered, which means that all the other

contributions have to be taken into account as well, and this assures the correct causality. The final result is of course the sum of all 4 contributions, as shown in figure 3.16. Apart from small modifications the result is similar to figure 3.12.

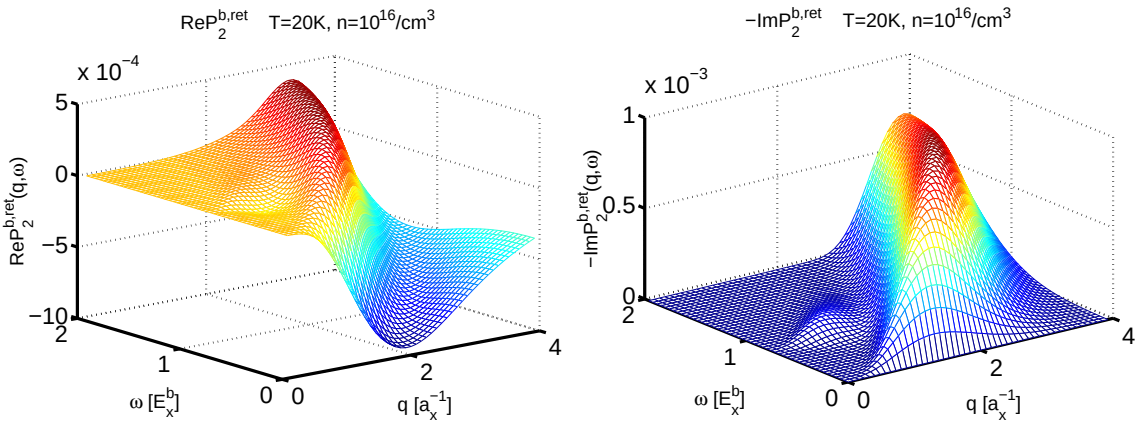

Figure 3.16: real and imaginary part of $P_2^{\mathrm{b,ret}}(q,\omega)$ as a function of wave vector q and energy ω and for $T = 20\mathrm{K}$(1s and 2s excitons considered)

Scattering Part

Now the scattering part of the two-particle polarisation function, given by (3.25) will be analysed. The results are given in figure 3.17. The graphs display the

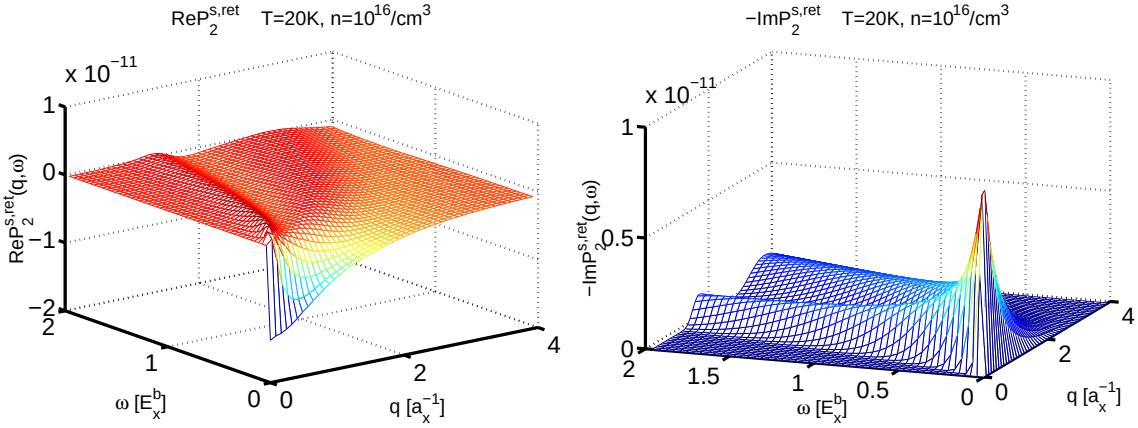

Figure 3.17: real and imaginary part of the scattering part of the two-particle polarisation function $P_2^{\mathrm{s,ret}}(q,\omega)$ as a function of wave vector q and energy ω and for $T = 20\mathrm{K}$

same characteristics as the results of the Lindhard polarisation function: there is an electron-pair continuum and a hole-pair continuum and there is also a contribution

to static screening. Comparing, however, the order of magnitude of the scattering part with the binding part, one obtains that the scattering contribution is smaller by a factor of $\approx 10^{-8}$ for the considered total density n and temperature T. Therefore, the scattering contribution to the two-particle polarisation function will be neglected in the following.
Summarising the results, it can be said, that the contribution of the bound states to the polarisation function is much bigger than that of the scattering states, and that within the fraction of the binding part $P^{\mathrm{b,ret}}_{2,11}(q,\omega)$ is the most important one. Comparing the one-particle polarisation function (figure 3.7) with the two-particle contribution, it is clear that for this temperature $T = 20\mathrm{K}$ and total density $n = 10^{16}/\mathrm{cm}^3$ the two-particle contribution is significant, i.e., excitonic screening is important!
This is directly coupled to the degree of ionisation α in the semiconductor and, for comparison, the one-particle polarisation function and the two-particle polarisation function are plotted in figure 3.18 and figure 3.19 for the same density but for the temperature $T = 77\mathrm{K}$, where the degree of ionisation is not $\alpha \approx 2 \cdot 10^{-3}$, but $\alpha \approx 0.65$, see also figure 2.4. The exciton fraction of the total density, which is

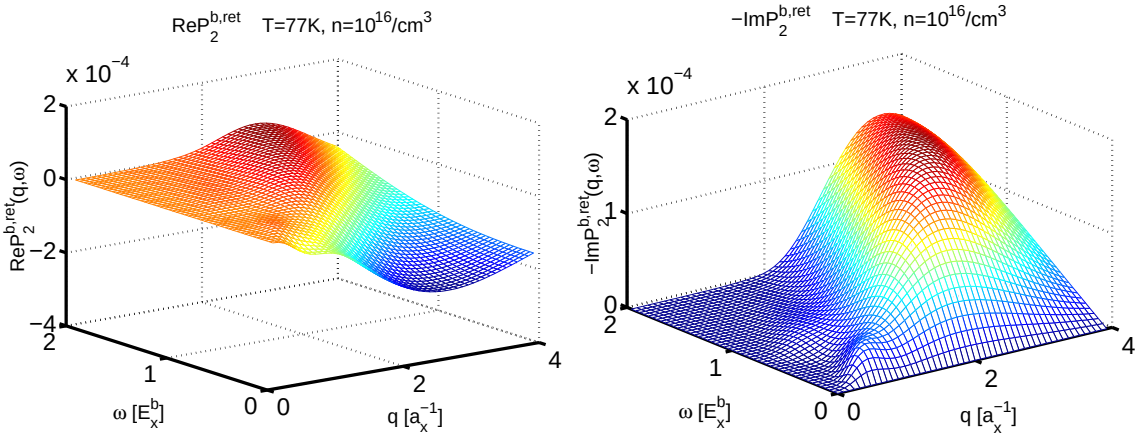

Figure 3.18: real and imaginary part of the binding part of the two-particle polarisation function $P^{\mathrm{b,ret}}_2(q,\omega)$ as a function of wave vector q and energy ω and for $T = 77\mathrm{K}$

$(1-\alpha)\cdot n$ has decreased from $T = 20\mathrm{K}$ to $T = 77\mathrm{K}$ by a factor of ≈ 3 and so the two-particle polarisation function has depleted by less than one order of magnitude. The free carrier fraction given by $\alpha \cdot n$ has increased, however, by a factor of ≈ 300 and consequently the single-particle polarisation function is amplified by more than two orders of magnitude, and is larger for these parameters than the two-particle contribution. Since the excitonic contributions to screening are of particular interest in this thesis the lower temperature is the more relevant one, when the diagonal dephasing $\Gamma_k(\omega)$ will be calculated, which is the aim of the next chapter.

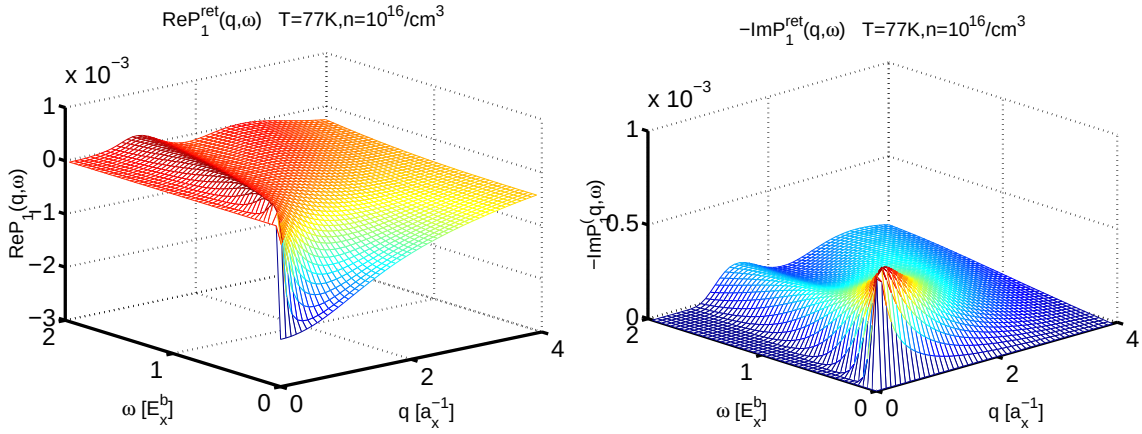

Figure 3.19: real and imaginary part of the one-particle polarisation function of a partially ionised plasma $P_1^{\mathrm{D,ret}}(q,\omega)$ as a function of wave vector q and energy ω and for $T = 77\mathrm{K}$

4 The Diagonal Dephasing

The dielectric properties of a semiconductor are determined by the susceptibility $\chi(\omega)$ which can be obtained experimentally by reflection and transmission measurements. In linear optical response it is connected to the macroscopic polarisation $P'(\omega)$, that is induced by the electromagnetic field $E(\omega)$ of a laser by

$$P'(\omega) = \chi(\omega)E(\omega)\,. \tag{4.1}$$

The polarisation can also be obtained theoretically by solving the Semiconductor Bloch equations (SBE). One important quantity in the SBE's is the diagonal dephasing $\Gamma_k(\omega)$ which is determined by many-body effects beyond the Hartree Fock approximation, and therefore influenced by the longitudinal polarisation function. The calculation of the diagonal dephasing, including the excitonic screening, is the aim of this chapter. After solving the SBE this can lead to a better agreement of theoretical and experimental results for the macroscopic polarisation, and to a better understanding of the experimentally obtained results.

4.1 Theory

In section 2.3.2 the Semiconductor Bloch equations were introduced, which are used for the calculation of the macroscopic polarisation $P'(t)$, that is induced by an external electromagnetic field, e.g. by a laser. In thermodynamical equilibrium and Fourier transformed into frequency space the equation for the polarisation was found to be

$$\begin{aligned}\left[\omega - \frac{\hbar^2 k^2}{2\mu} - \Delta_k^{\mathrm{HF}} - \Sigma_k^{\mathrm{c,ret}}(\omega) + i\gamma_0(\omega)\right] p_k(\omega) & \\ + \sum_q \left[N_k V_{k-q} + \Theta_{k,q}(\omega)\right] p_q(\omega) &= N_k d E(\omega)\,. \end{aligned} \tag{4.2}$$

The macroscopic polarisation is given by $P'(\omega) = \sum_k p_k(\omega)$. One quantity that influences the polarisation is the interband selfenergy $\Sigma^{\mathrm{ret}}(k,\omega)$, whose imaginary part is denoted as diagonal dephasing (the appearing quantities were explained in section 2.3.2). This diagonal dephasing is (in cooperation with other quantities) responsible for the decay of the laser-induced polarisation and given by the imaginary part of the retarded selfenergy $\Sigma^{\mathrm{ret}}(k,\omega)$, which is in quasiparticle (2.54) and linear

V^s approximation (2.43) (see [13])

$$\Sigma^{\mathrm{c,ret}}(k,\omega) = \sum_{a,b=e,h\ a\neq b} \int \frac{d^3q}{(2\pi)^3} \int \frac{d\omega'}{2\pi} \frac{\left[f_q^a + n(\omega')\right] 2\mathrm{Im}\{V_{k-q}^{\mathrm{s,ret}}(\omega')\}}{\omega' + \varepsilon_q^a + \varepsilon_k^b - \omega - i\left[\Gamma_q^a + \Gamma_k^b\right]}\,, \tag{4.3}$$

where $n(\omega)$ is Bose function $n(\omega) = \frac{1}{e^{\beta\omega}-1}$. ε_q^a is the renormalised single-particle energy $\varepsilon_q^a = \frac{\hbar^2q^2}{2m_a} - \mathrm{Re}\Sigma_q^{\mathrm{ret}}(\varepsilon_q^a)$ and Γ_q^a the single-particle damping, given by the imaginary part of the selfenergy in quasiparticle approximation $\Gamma_q^a = -2\mathrm{Im}\Sigma^{\mathrm{ret}}(\varepsilon_q^a)$ (2.55). The screened potential $V_k^{\mathrm{s,ret}}(\omega)$ is given by the bare Coulomb potential $V_k = \frac{8\pi}{k^2}$ (in excitonic units) and the dielectric function $\epsilon(k,\omega)$

$$V_k^{\mathrm{s,ret}}(\omega) = \frac{V_k}{\epsilon(k,\omega)}\,. \tag{4.4}$$

If only $k = 0$ is considered the integration over the angles ($V_{\mathbf{k-q}}^{\mathrm{s,ret}}(\omega)$!) becomes trivial and with (4.4) equation (4.3) can be simplified to

$$\Sigma_0^{\mathrm{ret}}(\omega) = \frac{4}{\pi} \sum_{a,b=e,h\ a\neq b} \int_0^\infty dq \int \frac{d\omega'}{2\pi} \frac{\left[f_q^a + n(\omega')\right] 2\mathrm{Im}\{\epsilon_q^{-1}(\omega')\}}{\omega' + \varepsilon_q^a + \varepsilon_0^b - \omega - i\left[\Gamma_q^a + \Gamma_0^b\right]}\,. \tag{4.5}$$

If furthermore the one-particle damping $\Gamma_q^a + \Gamma_0^b$ is replaced by an infinitesimal small damping constant δ the equation reduces to

$$\Sigma_0^{\mathrm{ret}}(\omega) = \frac{4}{\pi} \sum_{a,b=e,h\ a\neq b} \int_0^\infty dq \int \frac{d\omega'}{2\pi} \frac{\left[f_q^a + n(\omega')\right] 2\mathrm{Im}\{\epsilon_q^{-1}(\omega')\}}{\omega' + \varepsilon_q^a + \varepsilon_0^b - \omega - i\delta}\,, \tag{4.6}$$

and the imaginary part, which is the diagonal dephasing, can be obtained easily by using Dirac's identity (3.2)

$$\begin{aligned} \Gamma_0(\omega) &= -\mathrm{Im}\Sigma_0^{\mathrm{ret}}(\omega) \\ &= -\frac{4}{\pi} \sum_{a,b=e,h\ a\neq b} \int_0^\infty dq \left[f_q^a + n(\omega - \varepsilon_q^a - \varepsilon_0^b)\right] \mathrm{Im}\{\epsilon_q^{-1}(\omega - \varepsilon_q^a - \varepsilon_0^b)\}\,. \end{aligned} \tag{4.7}$$

A further simplification is to take the single-particle energies in the Debye approximation, given by (2.73), i.e.

$$\varepsilon_q^a + \varepsilon_0^b \approx \frac{\hbar^2q^2}{2m_a} - E_x^b\kappa a_x + 0 - E_x^b\kappa a_x = \frac{\hbar^2q^2}{2m_a} - 2E_x^b\kappa a_x\,, \tag{4.8}$$

which is in accordance with the consideration in the subsequent chapters. Finally, the imaginary part of the dielectric function can be given in terms of the polarisation function $P(q,\omega)$

$$\mathrm{Im}\epsilon_q^{-1}(\omega) = \frac{V_q\mathrm{Im}P(q,\omega)}{(1 - V_q\mathrm{Re}P(q,\omega))^2 + (V_q\mathrm{Im}P(q,\omega))^2}\,, \tag{4.9}$$

which is the link to the preceeding chapters. Having obtained results for the free carrier and the excitonic contribution to the polarisation function the diagonal dephasing can be calculated now taking into account free carrier screening, excitonic screening or both. The decisive question that can be answered then, is under which conditions the excitonic screening has significant influence on the diagonal dephasing and correspondingly on the macroscopic polarisation.
One remark concerning the used approximations: The Debye shift was a starting point in this thesis, and to assure consistency it has to be applied in every expression where a selfenergy shift is taken into account, although better approximations are possible. The neglection of the single-particle damping $\Gamma_q^a + \Gamma_0^b$ allows the direct evaluation of one frequency integral which simplifies the numerical implementation significantly. Furthermore, a finite damping would modify the results for the diagonal dephasing, but it would modify it for the one-particle contribution as well as for the two-particle contribution, consequently the question when excitonic screening is important can nevertheless be answered. To neglect the dependence of the diagonal dephasing on the wavevector is reasoned by experience. Further calculations show that the dependence is weak, see [13].

4.2 Results

Now the results for the diagonal dephasing Γ_0 will be presented. For an easy interpretation of the figures the plasma frequency ω_{pl} (3.14) and the inverse screening length κ (3.6) are given in excitonic units in the tabular below.

parameter	$T = 20\mathrm{K},\ n = 10^{16}/\mathrm{cm}^3$	$T = 77\mathrm{K},\ n = 10^{16}/\mathrm{cm}^3$
ω_{pl}	0.0071	0.126
κ	0.0258	0.230

Since the inverse screening length and the plasma frequency are proportional to $\sqrt{\alpha\, n}$, both parameters are much smaller for 20K, due to the low degree of ionisation.
In all following figures the x-axis is given as the energy difference to the bare band edge in units of the excitonic binding energy, i.e., $\omega = -1$ is the energy of the ground state exciton and $\omega = 0$ is the band edge of the nonexcited semiconductor. In fact the band edge of the considered excited semiconductor is shifted by many-body effects that are approximated here by the Debye shift, that means the band edge is supposed to be at $\omega = -2\kappa$.
Firstly, the results for the diagonal dephasing arising from the one-particle polarisation function P_1^D are computed. The superscript "D" stands for partially ionised system with Debye shift (2.73), i.e., the chemical potentials, which are parameters in the polarisation function, are obtained from Saha's equation (2.87).
In figure 4.1 the results for the diagonal dephasing $\Gamma_0(P_1^D)$ are displayed for $T = 77\mathrm{K}$ and $n = 10^{16}/\mathrm{cm}^3$ and, for comparison, in figure 4.2 the results for the same density

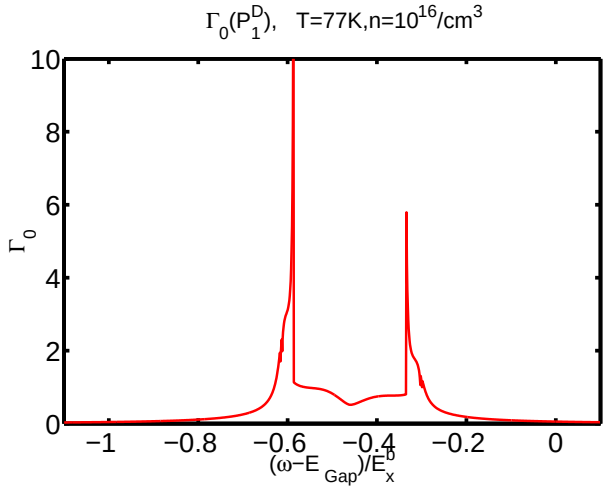

Figure 4.1: diagonal dephasing from pure single-particle screening $\Gamma_0(P_1^D)$ as a function of the energy ω at 77K

n and $T = 20$K. Clearly visible in all figures is the influence of the plasmon poles,

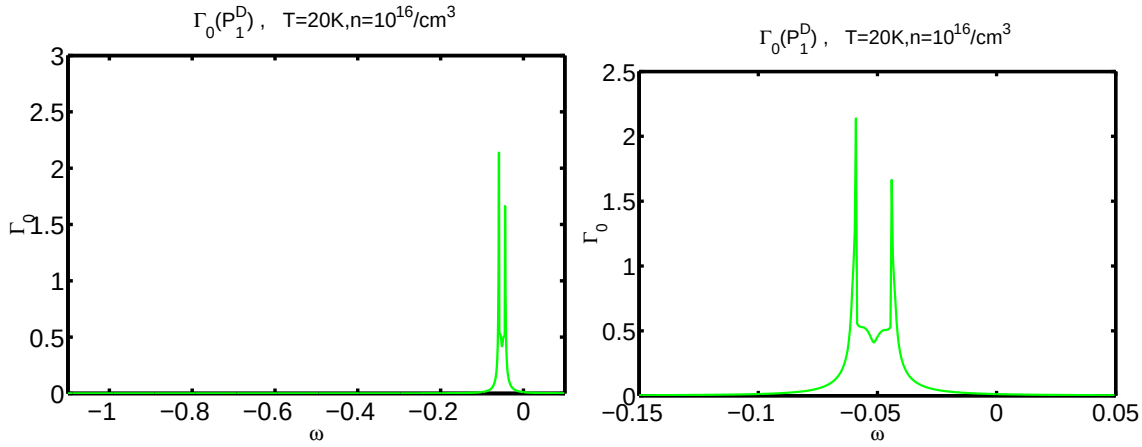

Figure 4.2: diagonal dephasing from pure single-particle screening $\Gamma_0(P_1^D)$ as a function of the energy ω at 20K,
left: same energy region as before right: range around the plasmon poles

which can be seen at $\omega = -2\kappa \pm \omega_{\mathrm{pl}}$. This means that at these energies the damping of the macroscopic polarisation P' is really high and, consequently, the decay of the induced polarisation is strong, which is in agreement with earlier calculations [17, 18, 19]. The plasmon poles are the roots of the dielectric function which is given here by the Lindhard polarisation formula (3.1). There they appear for frequencies at and slightly above the plasma frequency, see section 3.1.3 and figure 3.5 or 3.8. Since the imaginary part of the polarisation function vanishes for small transfer mo-

menta (see section 3.1 and figure 3.6) and no background damping was considered there and, furthermore, the one-particle damping in the diagonal dephasing was neglected, Γ_0 diverges at the frequencies of the plasmon poles $\omega = -2\kappa \pm \omega_{\mathrm{pl}}$. This means, in turn, that the higher the resolution of the graphs with respect to ω, the higher the peaks, therefore, one must not care too much about the absolute height of the diagonal dephasing at the plasmon poles. The height of the peaks is also influenced by the prefactors in (4.7) where $n(\omega)$ is the distribution function for the plasmons and, therefore, the peak at higher energies is smaller than the one at lower energies.
Now the diagonal dephasing Γ_0 is calculated, considering only the excitonic contribution to the polarisation function, given by (3.23). The results are displayed in figure 4.3, for better comparison splitted into the contributions arising from the different $P_{2,nn'}$. On the left Γ_0 is plotted on a logarithmic scale and one can obtain

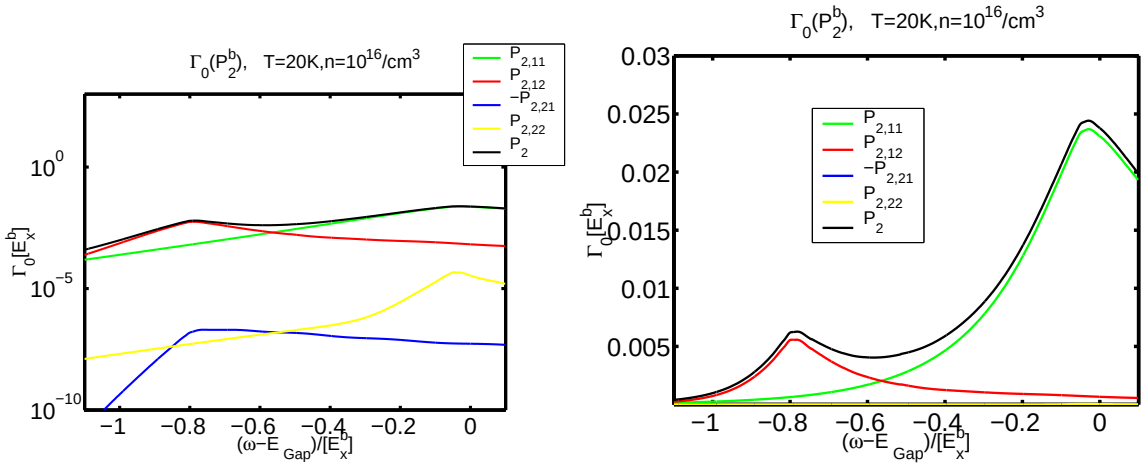

Figure 4.3: diagonal dephasing from pure excitonic screening $\Gamma_0(P_2)$ as a function of the energy ω at 20K,
left: logarithmic scale right: linear scale

that only the contributions from $P_{2,11}$ and $P_{2,12}$ are significant. On the right of figure 4.3 Γ_0 is plotted on a linear scale and it is visible that the influence of $P_{2,12}$ is most pronounced for $\omega \approx -0.80$. This is in accordance with figure 3.13 where the main peak in the imaginary part of the two-particle polarisation function is at $\omega \approx 0.75$ (the imaginary part of the two-particle polarisation function is, as the one-particle polarisation function, antisymmetric with respect to ω) and a Debye shift of $-2\kappa \approx -0.05$.
The same is true for $\Gamma_0(P_{2,21})$ (on a much smaller scale), but the contribution is negative, due to the different sign of $\mathrm{Im}P^b_{2,21}$, see figure 3.14. In the linear plot $\Gamma_0(P_{2,21})$ is not visible because it is covered by $\Gamma_0(P_{2,22})$. The main contributions of the diagonal elements of Γ_0 are around the shifted band edge $\omega = -2\kappa$, but as can be seen below, the influence of the one-particle contribution is clearly more important

at these energies.

For comparison, the diagonal dephasing caused by the free carriers and the pure excitonic contribution to it are displayed in figure 4.4, on the left for $T = 20$K, on the right for $T = 77$K. In both figures is visible that, in the area around the

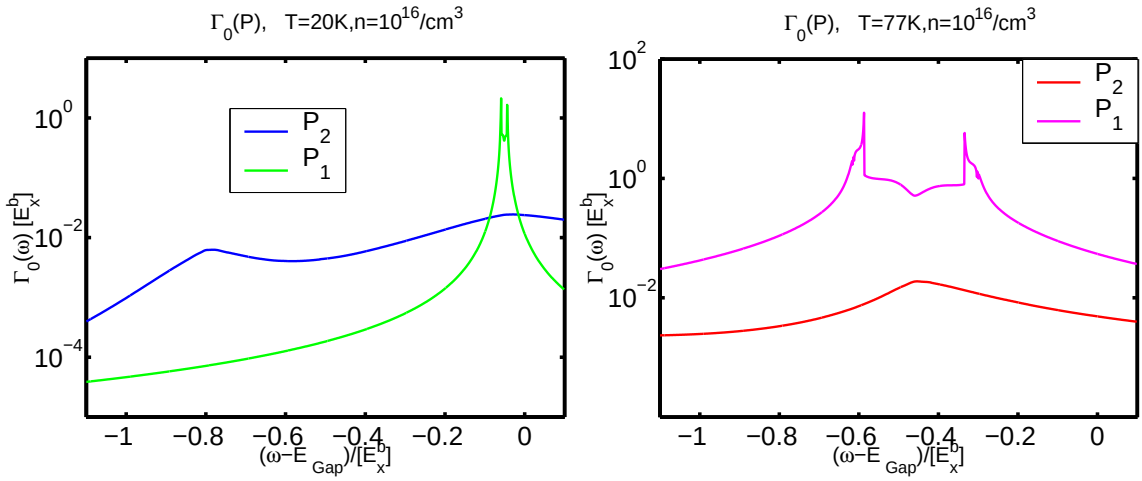

Figure 4.4: one-particle and two-particle contribution to Γ_0 as a function of the energy ω
left:$T = 20$K, right: $T = 77$K

(shifted) band edge $\omega = -2\kappa$, the single-particle screening contribution is superior, while for other energies the relative importance depends on the temperature (via the degree of ionisation). For $T = 77$K the diagonal dephasing Γ_0 due to the free carriers is at least one order of magnitude larger than the excitonic contribution over the whole energy range, while for $T = 20$K the diagonal dephasing arising by the excitonic screening is orders of magnitude larger for energies well below the plasmon pole peaks.
Actually, the total diagonal dephasing, calculated from the total polarisation function

$$P^{\mathrm{ret}}(q,\omega) = P_1^{\mathrm{D,ret}}(q,\omega) + P_2^{\mathrm{ret}}(q,\omega)\,, \tag{4.10}$$

(where P_2 is only the bound part) is not the sum of the one-particle and the two-particle contribution, but given by (4.7), which is an integral over the imaginary part of the dielectric function (4.9). The results for the total diagonal dephasing are given in figure 4.5. Since the two-particle polarisation function does not contribute in the area where the one-particle polarisation function has the plasmon poles the influence of the plasmon poles on the diagonal dephasing is not modified visibly. In general it can be said that one-particle screening dominates around the shifted band edge with strongly decreasing tails, while for energies below, the excitonic screening is of more importance. The linewidth (i.e. the life time) of a ground state exciton with

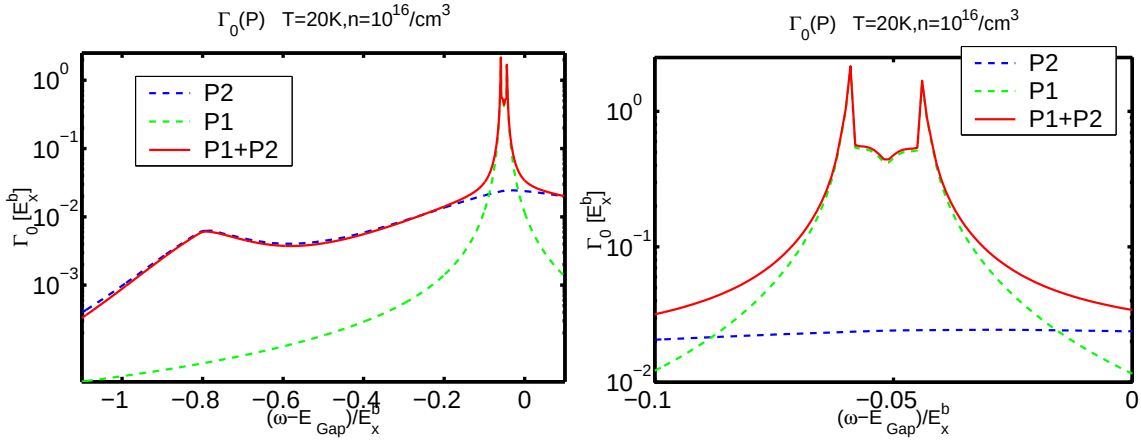

Figure 4.5: diagonal dephasing Γ_0 as a function of the energy ω

energy $E = -E_x^b$ depends on the diagonal dephasing at this energy, this means that the excitonic linewidth increases because of excitonic screening. Since the linewidth of the ground state exciton is (indirectly) measurable, the experimental results may correspond better to the now improved theory.
One may wonder why the total diagonal dephasing is smaller for some values than the two-particle contribution to it, this is, however, reasoned by the complicated relation between the polarisation function and the diagonal dephasing. For certain energy- and momentum-transfer values $\mathrm{Re}P_1$ and $\mathrm{Re}P_2$ have different signs, which can mean that the total inverse dielectric function is smaller than the two-particle contribution to it, which in turn leads to the obtained result.
The results for $T = 77\mathrm{K}$ are not shown, because as can already be seen in figure 4.4, the total diagonal dephasing is dominated by the single-particle contribution.

The final result of this chapter is that the diagonal dephasing Γ_0, which influences the macroscopic polarisation P', is modified considerably by excitonic screening in a system with a low degree of ionisation. Furthermore, the linewidth of excitons (especially ground state excitons) is controlled more by two-particle screening than by one-particle screening. This means that for low temperatures the consideration of screening by the Lindhard formula is not sufficient, but excitonic screening has to be taken into account as well.

5 Conclusion

5.1 Summary

An improved description of screening was the aim of this thesis. Screening is a many-body effect, arising due to the long-range Coulomb interaction of charge carriers in a semiconductor with surrounding charge carriers. The properties of the charge carriers in the system, like their dispersion relation and the lifetime are modified significantly by screening, which motivates its investigation.
In chapter 2 the general properties of an excited semiconductor were analysed and the theoretical base for continuative considerations was found. In particular, the systematic treatment of many-body problems with Green's functions was explained in section 2.3. Of further interest were the properties of an interacting and partially ionised Coulomb plasma in a semiconductor, i.e., a system consisting of electrons, holes and excitons. With the help of Saha's equation (2.87) the influence of the parameters temperature and total density on the degree of ionisation and the chemical potentials was investigated in section 2.4. To be able to evaluate the influence of excitons on screening one parameter set corresponding to a system with a high degree of ionisation and one parameter set corresponding to a system with low degree of ionisation were chosen. At a total density of $n = 10^{16}/\mathrm{cm}^3$ and a temperature of $T = 77\mathrm{K}$ the degree of ionisation was found to be $\alpha \approx 0.65$ while for the same density, but a temperature of $T = 20\mathrm{K}$ the degree of ionisation was calculated to $\alpha \approx 0.002$, which means that 99.8% of all electrons and holes are bound to excitons for these parameters.
The polarisation function was in the focus of chapter 3. Firstly the free carrier polarisation function (3.1) was analysed, for an ideal Coulomb plasma as well as for an interacting plasma, and secondly the excitonic polarisation (3.23,3.25) function was calculated and evaluated. Since the polarisation function depends crucially on the degree of the ionisation the excitonic contribution to it was found to be larger than the free carrier contribution for an excited semiconductor at low temperature and thus low degree of ionisation. In contrast to this the free carrier screening is more important for higher temperatures and higher degrees of ionisation. Furthermore, it was found that the binding part of the two-particle polarisation function goes to zero for vanishing transfer momentum and transfer energy, which means that it makes no contribution to the static and the long wavelength limit of the polarisation function. After calculating the scattering part of the two-particle polarisation function it was found to be neglectable in comparison with the binding part, which means that only

excitons are important for two-particle screening.
The next step, done in chapter 4, was to study the result of the improved screening on the properties of the charge carriers in the semiconductor. Investigating therefore the diagonal dephasing, which is one of the quantities influencing the macroscopic polarisation, and comparing the results, obtained with and without excitonic screening, significant differences were found for a system with a low degree of ionisation. While in the vicinity of the band edge the diagonal dephasing is governed by single-particle screening, especially by plasmons, which are the elementary single-particle excitations, in the energetic region well below the band edge it is crucially increased by two-particle screening. This leads, for example, to an amplified spectral linewidth of the ground state excitons, corresponding to a reduced life time.
In general it can be concluded, that for excited semiconductors, where the parameters are chosen in a way that the degree of ionisation of the electron-hole plasma is low, the consideration of excitonic screening is necessary.

5.2 Outlook

Since many-body physics was considered in this thesis, many approximations were applied. Probably the first thing to improve is the influence of the system on the one-particle states. The kinetic energy of these states was assumed to be modified by the Debye shift (2.73) and no damping was included. An reasonable improvement is to apply the quasiparticle approximation(2.54), which would include a finite damping of the one-particle states and the replacement of the oversimplifying Debye shift by the sum of a Hartree-Fock and a correlation shift. The expected results are a damping of the diagonal dephasing at the plasmon poles and a slower decrease of the tails. Furthermore, the calculation of the diagonal dephasing including the wavevector dependence is aimed for.
Another point is the comparison of the obtained results with experimental data. One possibility might be the experimental determination of the macroscopic polarisation of an excited semiconductor for a constant excitation density n, but varying temperature. Going from high to low temperature this would correspond to a decrease of the degree of ionisation (figure 2.4) and therefore with an expected increase of the importance of excitonic screening. Comparing theoretical predictions with experimental measurements, the importance of this thesis might be proven.

5.3 Numerics

Due to the complexity of the involved equations, many results were obtained with the help of a computer. All routines are self-written in “C” (except one tiny function for a polynomial interpolation) and were tested various times by limiting cases or simplifications. The figures of this thesis were designed with “MatLab” and some

calculations were done with “Mathematica”.

5.4 List of Used symbols

For a clear arrangement, (almost) all labels are given in two tabulars below. The first one for the Latin letters and the second one for the Greek.

symbol	quantity
a, b, c	particle sort index
d	dipole matrix element
e	elementary charge, electron
E	(kinetic) energy
f_k^a	Fermi function, possibly also with a modified dispersion relation
g_k^a	Bose function, possibly also with a modified dispersion relation
h	hole
$\hbar$	Planck’s constant over 2π
Im	imaginary part
k	wave vector, also denoted as momentum
k_b	Boltzmann’s constant
m_a	effective carrier mass
m_0	free electron mass
M	total mass (of a two-body system)
n	principal quantum number, (total) particle density
n_a	free particle density
p	wave vector, also denoted as momentum
p_k	element of the macroscopic polarisation P'
P	polarisation function
P'	macroscopic polarisation
q	(transfer) wave vector
Re	real part
T	temperature, T-matrix
x	exciton

symbol	quantity
α	degree of ionisation
α_a	particle mass factor $\alpha_a = \mu/m_a$
α'	exciton mass factor $\alpha' = \mu/(m_e + m_h)$
β	inverse temperature $\beta = 1/k_b T$
γ	background damping
Γ	damping
Γ_0	diagonal dephasing
δ	infinite element
ϵ_0	dielectric constant
ϵ_r	relative permeability
ε	modified kinetic energy
$\theta_{q,k}$	effective interaction matrix
κ	inverse screening length, Debye shift in excitonic units
μ	reduced mass of electron and hole
μ_a	chemical potential of particle type a
μ_x	exciton chemical potential
ν	band index
Σ	(interband) selfenergy
ψ	excitonic wave function
ω, Ω	energy, also denoted as frequency

A Units and Applied Conventions

To get values easy to manage it is often useful to express physical quantities in the natural units of a system. Therefore, all numerical results will be given in excitonic units, except for temperature and density, for which SI units will be used. Fundamental calculation will also be done in SI units, while for applied ones results in excitonic units are often more descriptive.

The natural energy unit of an excited semiconductor is the excitonic Rydberg energy E_x^b which is defined similar to the Rydberg constant in hydrogen

$$E_x^b = \frac{e^4 \mu}{2(4\pi\epsilon_0\epsilon_r\hbar)^2} \tag{A.1}$$

and is the binding energy of an 1s exciton. The reduced mass μ is given by the electron and hole masses. For ZnSe the binding energy

$$E_x^b = 0.0224\text{eV} \tag{A.2}$$

The other used natural unit is the excitonic Bohr radius a_x, which is again defined analogue to the hydrogen Bohr radius

$$a_x = \frac{\hbar^2 4\pi\epsilon_0\epsilon_r}{e^2\mu} = 3.648 \cdot 10^{-9}\text{m} \tag{A.3}$$

and much larger than in hydrogen, because the binding energy is weaker. With the last equation E_x^b can be rewritten as

$$E_x^b = \frac{\hbar^2}{2\mu a_x^2}\,. \tag{A.4}$$

The particle masses can be expressed by mass factors

$$\alpha_a = \frac{\mu}{m_a}. \tag{A.5}$$

This is useful because now every physical value can be expressed in excitonic units. As an example the kinetic energy of particles type a can be transformed from SI to excitonic units as follows

$$E_{\text{kin}}^a = \frac{k^2\hbar^2}{2m_a} = \frac{k^2\hbar^2}{2\mu} \cdot \frac{\mu}{m_a} = E_x^b a_x^2 k^2 \alpha_a = \alpha_a \tilde{k}^2 \tag{A.6}$$

The last step can be done because the excitonic constants are "1" in excitonic units. The tildes are omitted throughout this thesis for simplicity.
Other often used transformation are

physical value	SI	excitonic units
bare Coulomb potential V_k	$\frac{e^2}{\epsilon_0 k^2}$	$\frac{8\pi}{k^2}$
Debye Potential V^{D}	$\frac{e^2}{\epsilon_0(k^2+\kappa^2)}$	$\frac{8\pi}{k^2+\kappa^2}$

Where energies are given by $E = \hbar\omega$, the prefactor $\hbar$ is omitted for laziness throughout the thesis. Furthermore vectors (indicated by bold type) are omitted, except where the vector character is important. Most equations however, are scalar equations.

B The Selfenergy in Quasi-Particle Approximation

The aim of this derivation is managable expression for the selfenergy in linear-V^s and quasi-particle approximation. It holds

$$\Sigma_a(k,\omega)^{\rm ret} = \int \frac{d\omega'}{2\pi} \frac{\Sigma_a^>(k,\omega') - \Sigma_a^<(k,\omega')}{\omega - \omega' + i\delta}\,, \tag{B.1}$$

$$\Gamma_k(\omega) = {\rm Im}\Sigma_a(k,\omega)^{\rm ret} = \Sigma_a^>(k,\omega) + \Sigma_a^<(k,\omega)\,, \tag{B.2}$$

while the greater/smaller components of the selfenergy are given by

$$\Sigma_a^{\gtrless}(k,\omega) = \sum_q \int \frac{d\omega'}{2\pi} G_a^{\gtrless}(k-q,\omega-\omega') V^{s,\gtrless}(q,\omega')\,. \tag{B.3}$$

In section 2.3.1 some properties of Green's functions were introduced

$$G_a^<(k,\omega) = f^a(\omega)\hat{G}_a(k,\omega)\,, \tag{B.4}$$

$$G_a^>(k,\omega) = (1-f^a(\omega))\hat{G}_a(k,\omega)\,, \tag{B.5}$$

$$\hat{G}_a(k,\omega) = -2{\rm Im}G_a^{\rm ret}(k,\omega)\,. \tag{B.6}$$

The retarded single-particle Green's function in quasi-particle approximation is (2.54)

$$G_a^{\rm ret}(k,\omega) = \frac{1}{\omega - \varepsilon_k^a + i\Gamma_k^a/2}\,, \tag{B.7}$$

thus one obtaines

$$G_a^<(k,\omega) = f^a(\omega)\frac{\Gamma_k^a}{(\omega-\varepsilon_k^a)^2 + (\Gamma_k^a/2)^2}\,, \tag{B.8}$$

$$G_a^>(k,\omega) = (1-f^a(\omega))\frac{\Gamma_k^a}{(\omega-\varepsilon_k^a)^2 + (\Gamma_k^a/2)^2}\,. \tag{B.9}$$

Calculating now the imaginary part of the selfenergy in quasi-particle approximation ($\Gamma_k(\omega) \to \Gamma_k(\varepsilon_k^a)$) one obtaines:

$$\begin{aligned}
\Gamma_k(\varepsilon_k^a) &= \Sigma_a^>(k,\omega) + \Sigma_a^<(k,\omega)\,, && \text{(B.10)}\\
&= \sum_q \int \frac{d\omega'}{2\pi} G_a^>(k-q, \varepsilon_k^a - \omega') V^{s,>}(q,\omega') \\
&+ \qquad\qquad G_a^<(k-q, \varepsilon_k^a - \omega') V^{s,<}(q,\omega') && \text{(B.11)}\\
&= \sum_q \int \frac{d\omega'}{2\pi} \frac{\Gamma_{k-q}^a}{(\varepsilon_k^a - \omega' - \varepsilon_{k-q}^a)^2 + (\Gamma_{k-q}^a/2)^2} \\
&\cdot \left[(1 - f^a(\varepsilon_k^a - \omega')) V_q^{s,>}(\omega') + f^a(\varepsilon_k^a - \omega') V_q^{s,<}(\omega')\right]\,. && \text{(B.12)}
\end{aligned}$$

The selfenergy is then given as

$$\sum_q \int \frac{d\omega'}{2\pi} \frac{\left[(1 - f^a(\varepsilon_k^a - \omega')) V_q^{s,>}(\omega') + f^a(\varepsilon_k^a - \omega') V_q^{s,<}(\omega')\right]}{-\varepsilon_k^a + \omega' + \varepsilon_{k-q}^a - i\Gamma_{k-q}^a/2}\,. \qquad \text{(B.13)}$$

Redefining $k-q =: q' \to q$ and therefore changing the sign the final result is obtained

$$\Sigma_a^{\mathrm{c,ret}}(k, \varepsilon_a(k)) = \sum_q \int \frac{d\omega}{2\pi} \frac{[1 - f_q^a] V_{k-q}^{s,>}(\omega) - f_q^a V_{k-q}^{s,<}(\omega)}{\varepsilon_k^a - \varepsilon_q^a - \omega - i\Gamma_q^a/2}\,. \qquad \text{(B.14)}$$

C The Lindhard Polarisation Formula

The one-particle approximation for the polarisation is the Lindhard function

$$P(q,\omega) \approx P_1(q,\omega)^{\mathrm{ret}} = 2\sum_{a=e,h}\int \frac{d^3k}{(2\pi)^3}\frac{f^a(k)-f^a(k-q)}{\omega - e^a(k)+e^a(k-q)+i\delta} \tag{C.1}$$

$f^a(k)$ is the Fermi function of a particle with type a and momentum k, $e^a(k)$ stands for the single particle energy.

Equation (3.1) can be developed with the help of Green's function technique. The polarisation function is defined as the partial sum of all diagrams contained in the self energy that do not split after cutting one line of interaction.

The simplest approximation is to consider the first diagram only, i.e. one has to evaluate only two one-particle Green functions. Using the Matsubara technique (

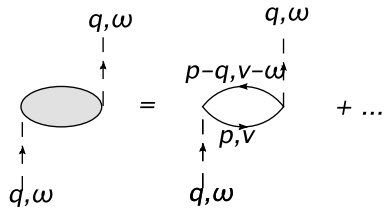

Figure C.1: Lindhard approximation for the polarisation

an introduction is given for example in [3]) the frequencies are taken imaginary, i.e.

$$\nu \to iz_\nu; \quad \omega \to iz_\mu\,.$$

p and iz_ν are the internal variables that have to be summed up, while q and iz_μ are the external variables from the polarisation. The Matsubara frequencies are defined as

$$z_a = \frac{\pi n}{\beta}, \tag{C.2}$$

where n is odd for fermionic frequencies like z_ν and even for bosonic ones like z_μ. Considering the spin and other prefactors correctly one can read from diagram C.1

$$P_1(q,iz_\mu) = \frac{-2}{\beta}\sum_{p,\nu} g_0(p+q,iz_\nu+iz_\mu)\cdot g_0(p,iz_\nu) \tag{C.3}$$

One can insert now the single particle green functions

$$g_0(p, iz_\nu) = \frac{1}{iz_\nu - e_p} = \frac{1}{iz_\nu - (\frac{p^2}{2m} - \mu)} \tag{C.4}$$

obtaining

$$P_1(q, iz_\mu) = \frac{2}{\beta} \sum_{p,\nu} \frac{1}{iz_\nu + iz_\mu - e_{p+q}} \frac{1}{iz_\nu - e_p} \tag{C.5}$$

A great advantage of the Matsubara technique is that the frequency summation can be transformed into a complex integration, which can be executed easily.

$$\sum_\nu h(iz_\nu) = -\frac{\beta}{2\pi i} \int_C dz f(z) h(z) \tag{C.6}$$

The reason for this equation is that the Matsubara frequencies are the roots of the complex Fermi funtion $f(z)$. One gets

$$P_1(q, iz_\mu) = \frac{-2}{2\pi i} \sum_p \int_C f(z) \frac{1}{z + iz_\mu - e_{p+q}} \frac{1}{z - e_p} \tag{C.7}$$

One can evaluate the complex integral with the theorem for residues

$$\int_C h(z) dz = 2\pi i \sum \text{Res} \tag{C.8}$$

but to get the residues (prefactors of the poles) an expansion into partial fractions is performed.

$$\begin{aligned} P_1(q, iz_\mu) &= \frac{-2}{2\pi i} \sum_p \int_C dz f(z) \frac{1}{z + iz_\mu - e_{p+q}} \frac{1}{z - e_p} && \text{(C.9)} \\ &= \frac{-2}{2\pi i} \sum_p \int_C \frac{dz f(z)}{\epsilon_p - e_{p+q} + iz_\mu} \left[\frac{-1}{z + iz_\mu - e_{p+q}} + \frac{1}{z - e_p} \right] && \text{(C.10)} \\ &= 2 \sum_p \frac{-f(-iz_\mu + e_{p+q}) + f(e_p)}{e_p - e_{p+q} + iz_\mu} && \text{(C.11)} \\ &= 2 \sum_p \frac{-f(e_{p+q}) + f(e_p)}{e_p - e_{p+q} + iz_\mu} && \text{(C.12)} \end{aligned}$$

In the last step was used that $z_\mu = \frac{\pi n}{\beta} \quad n = 0, \pm 2...$ is a bosonic Matsubara frequency, i.e. $f(iz_\mu + e_p) = f(e_p)$.
The chemical potentials contained in ϵ_p cancel in the denominator and finally after writing the sum over p as an integral, summing up over both particle types and transforming the imaginary frequency back into a real and retarded one

$$iz_\mu \to \omega + i\delta$$

the Lindhard formula for the polarisation is obtained.

$$P_1^{\mathrm{ret}}(q,\omega) = 2\sum_{a=e,h}\int \frac{d^3k}{(2\pi)^3}\frac{f^a(k)-f^a(k-q)}{\omega - e^a(k)+e^a(k-q)+i\delta} \tag{C.13}$$

D The Lindhard Formula for Ideal and Interacting Systems

In the non-degenerated limit it can be shown that for all q and ω that the ratio of the real parts of the single particle Polarisation function of an ideal system $ReP_1^0(q,\omega)$ and of an interacting one $ReP_1^D(q,\omega)$is simply given by the degree of ionisation α

$$\frac{ReP_1^0(q,\omega)}{ReP_1^D(q,\omega)} = \frac{1}{\alpha} \tag{D.1}$$

Performing the integration over the angles and applying excitonic units, the real part can be written as

$$\begin{aligned} ReP_1(q,\omega) &= 2\sum_{a=e,h}\int \frac{d^3k}{(2\pi)^3}\frac{f^a(k)-f^a(k-q)}{\omega - e^a(k)+e^a(k-q)} && \text{(D.2)}\\ &= \frac{1}{4\pi^2}\sum_{a=e,h}\frac{1}{\alpha_a}\int_{-\infty}^{\infty} dkkf^a(k)\ln\frac{|k-\omega_q^-|}{|k-\omega_q^+|} && \text{(D.3)}\\ \text{with } \omega_q^{\pm} &= \frac{\omega \pm \alpha_a q^2}{2\alpha_a q} && \text{(D.4)} \end{aligned}$$

This means that

$$\begin{aligned} \frac{ReP_1^0(q,\omega)}{ReP_1^D(q,\omega)} &= \frac{\sum_{a=e,h}\frac{1}{\alpha_a}\int_{-\infty}^{\infty} dkkf^{a,0}(k)\ln\frac{|k-\omega_q^-|}{|k-\omega_q^+|}}{\sum_{a=e,h}\frac{1}{\alpha_a}\int_{-\infty}^{\infty} dkkf^{a,D}(k)\ln\frac{|k-\omega_q^-|}{|k-\omega_q^+|}} && \text{(D.5)}\\ &\approx \frac{\sum_{a=e,h}e^{\beta\mu_a^0}\frac{1}{\alpha_a}\int_{-\infty}^{\infty} dkke^{-\beta\alpha_a k^2}\ln\frac{|k-\omega_q^-|}{|k-\omega_q^+|}}{\sum_{a=e,h}e^{\beta(\kappa+\mu_a^D)}\frac{1}{\alpha_a}\int_{-\infty}^{\infty} dkke^{-\beta\alpha_a k^2}\ln\frac{|k-\omega_q^-|}{|k-\omega_q^+|}} && \text{(D.6)} \end{aligned}$$

after applying the Boltzmann limit to the Fermi functions of the ideal and the interacting system, where the latter one include a Debye shift of $\Delta_a = -\kappa$.

$$f^{a,0}(k) = \frac{1}{e^{\beta(\alpha_a^2k^2-\mu_a^0)}+1} \quad ; f^{a,D}(k) = \frac{1}{e^{\beta(\alpha_a^2k^2-\kappa-\mu_a^D)}+1} \tag{D.7}$$

The chemical potentials can be calculated in the Boltzmann case analytically from the equation of state

$$\mu_a^0 = \frac{1}{\beta}\ln\left(\frac{n\lambda^3}{2}\right) \quad \mu_a^D = \frac{1}{\beta}\ln\left(\frac{n\alpha\lambda^3}{2}\right) - \kappa \tag{D.8}$$

$$\text{with} \quad n_a^0 = n \quad n_a^D = \alpha n \ \text{ densities} \tag{D.9}$$

so, after inserting the chemical potentials one receives the expected result.

$$\frac{ReP_1^o(q,\omega)}{ReP_1^n(q,\omega)} = \frac{\sum_{a=e,h} \frac{\lambda_a^3 n}{2} \frac{1}{\alpha_a} \int_{-\infty}^{\infty} dkke^{-\beta\alpha_a k^2} \ln \frac{|k-\omega_q^-|}{|k-\omega_q^+|}}{\sum_{a=e,h} \frac{\lambda_a^3 \alpha n}{2} \frac{1}{\alpha_a} \int_{-\infty}^{\infty} dkke^{-\beta\alpha_a k^2} \ln \frac{|k-\omega_q^-|}{|k-\omega_q^+|}} \tag{D.10}$$

$$= \frac{\sum_{a=e,h} \frac{\lambda_a^3 n}{2} \frac{1}{\alpha_a} \int_{-\infty}^{\infty} dkke^{-\beta\alpha_a k^2} \ln \frac{|k-\omega_q^-|}{|k-\omega_q^+|}}{\alpha \sum_{a=e,h} \frac{\lambda_a^3 n}{2} \frac{1}{\alpha_a} \int_{-\infty}^{\infty} dkke^{-\beta\alpha_a k^2} \ln \frac{|k-\omega_q^-|}{|k-\omega_q^+|}} \tag{D.11}$$

$$= \frac{1}{\alpha} \tag{D.12}$$

Furthermore it can be shown that this result holds true also for the degenerated case for the static and long wavelength limit.
For the imaginary part no such relation can be given.

Acknowledgements

There are some people I would like to thank for their support. My special and emphatic thanks go to Dr. Günter Manzke and Dr. Tim Schmielau.
The former one I'd like to thank for uncounted patient and comprehensible explanations of physical problems and the latter one for overwhelming helpfulness in physical as well as in numerical questions. Furthermore I'd like to thank Tim for always destroying my with much effort self-built theories and models and afterwards showing me that everything is much more complicated than I assumed it to be, because it keeps my brain busy.

Additionally I wish to thank Prof. Henneberger for the opportunity to write this thesis and the chance to get some insight in semiconductor physics. Likewise I'm really thankful to Dr. Dirk Semkat and the three already mentioned for reading various drafts of this thesis over and over again and giving valuable comments on it. I would like to thank the work group in general for the relaxed and cooperative atmosphere, which I really like.

The last but one greeting goes to my fellow students, especially Michi and Alex, who I enjoyed the exciting experiences of my studies with.

The very last idea goes out to my beloved fiancée, who always brings me back to reality and shares the real important things in live with me.

Bibliography

[1] J. Lindhard, K. Dan. Vidensk Selsk. Mat-Fys Medd **28**, Nr 8 (1954)

[2] H.Haug and S.Koch *Quantum Theory of the Optical and Electronic Properties of Semiconductors*, (World Scientific Publishing, 2004)

[3] W.-D. Kraeft, D.Kremp, W.Ebeling, and G.Röpke *Quantum Statistics of Charged Particle Systems*, (Akademie-Verlag Berlin, 1986)

[4] G.D. Mahan *Many-Particle Physics*, (Plenum Press New York, 1993)

[5] G. Röpke and D.Der *The Influence of Two-Particle States (Excitons) on the Dielectric Function of the Electron-Hole Plasma*, phys. stat. sol (b) **92**, 501 (1979)

[6] G. Manzke, V. May and K. Henneberger, *Excited States and Collective Excitations in a Dense Gas of Excitons*, phys. stat. sol (b) **125**, 693 (1984)

[7] M. Lindberg and S.W. Koch, Phys. Rev. B **38**, 3342 (1988)

[8] N.W. Ashcroft and N.D. Mermin, *Solid State Physics*, (Brooks Cole 1976)

[9] http://www.britneyspears.ac/lasers.htm

[10] D.Kremp, M.Schlanges, and W.-D. Kraeft *Quantum Statistics of Nonideal Plasmas*, (Springer Verlag Berlin Heidelberg, 2005)

[11] K. Henneberger, H. Haug, *Nonlinear optics and transport in laser–exited semiconductors*, Phys. Rev. B **38**, 9759 (1988)

[12] G. Manzke, Q.Y Peng, K. Henneberger, U. Neukirch, K. Hauke, K. Wundke, J. Gutowski, and D. Hommel, Phys. Rev. Lett. **80**, 4943 (1998)

[13] J.S. Nägerl, B. Stabenau, G. Böhne, S. Dreher, R.G. Ulbrich, G. Manzke, and K. Henneberger, *Polariton pulse propagation through GaAs: Excitation-dependent phase shifts*, Phys. Rev. B, **63**, 235202-1 (2001)

[14] R. Zimmermann *Many-Particle Theory of Highly Excited Semiconductors*, (B.G. Teubner Verlagsgesellschaft Leipzig, 1988)

[15] D.W. Snoke and J.D. Crawford, *Hysteresis in the Mott transition between plasma and insulating gas*, Phys. Rev. E **52**, 5796 (1995)

[16] D. Kremp, M. Schlanges, and T. Bornath, *Kinetic Theory of Chemically Reacting Systems*, phys. stat. sol. (b) **147**, 747 (1988)

[17] T. Schmielau *Optische und Ein-Teilchen-Eigenschaften von Halbleitern*, Dissertation, (Rostock, 2001)

[18] U.v. Bart, B. Holm *Self-consistent GW_0 results for the electron gas: Fixed screened potential W_0 within the random phase approximation*, Phys. Rev. B **54**, 8411 (1995)

[19] U.v. Bart and B. Holm *Erratum: Self-consistent GW_0 results for the electron gas: Fixed screened potential W_0 within the random phase approximation*, Phys. Rev. B **54**, 8411 (1996)

Erklärung

Hiermit versichere ich, daß ich die vorliegende Arbeit selbständig angefertigt und ohne fremde Hilfe verfaßt, keine außer den von mir angegebenen Hilfsmitteln und Quellen dazu verwendet und die den benutzten Werken inhaltlich und wörtlich entnommenen Stellen als solche kenntlich gemacht habe.

Rostock, September 2006